Feasibility, Safety, and Therapeutic Efficacy of Human Induced Pluripotent Stem Cell-Derived Cardiomyocyte Sheets in a Porcine Ischemic Cardiomyopathy Model

Masashi Kawamura, MD; Shigeru Miyagawa, MD, PhD; Kenji Miki, MSc; Atsuhiro Saito, PhD; Satsuki Fukushima, MD, PhD; Takahiro Higuchi, MD; Takuji Kawamura, MD; Toru Kuratani, MD, PhD; Takashi Daimon, PhD; Tatsuya Shimizu, MD, PhD; Teruo Okano, PhD; Yoshiki Sawa, MD, PhD

Background—Human induced pluripotent stem cell-derived cardiomyocytes (hiPS-CMs) are a promising source of cells for regenerating myocardium. However, several issues, especially the large-scale preparation of hiPS-CMs and elimination of undifferentiated iPS cells, must be resolved before hiPS cells can be used clinically. The cell-sheet technique is one of the useful methods for transplanting large numbers of cells. We hypothesized that hiPS-CM-sheet transplantation would be feasible, safe, and therapeutically effective for the treatment of ischemic cardiomyopathy.

Methods and Results—Human iPS cells were established by infecting human dermal fibroblasts with a retrovirus carrying Oct3/4, Sox2, Klf4, and c-Myc. Cardiomyogenic differentiation was induced by WNT signaling molecules, yielding hiPS-CMs that were almost 90% positive for α-actinin, Nkx2.5, and cardiac troponin T. hiPS-CM sheets were created using thermoresponsive dishes and transplanted over the myocardial infarcts in a porcine model of ischemic cardiomyopathy induced by ameroid constriction of the left anterior descending coronary artery (n=6 for the iPS group receiving sheet transplantation and the sham-operated group; both groups received tacrolimus daily). Transplantation significantly improved cardiac performance and attenuated left ventricular remodeling. hiPS-CMs were detectable 8 weeks after transplantation, but very few survived long term. No teratoma formation was observed in animals that received hiPS-CM sheets.

Conclusions—The culture system used yields a large number of highly pure hiPS-CMs, and hiPS-CM sheets could improve cardiac function after ischemic cardiomyopathy. This newly developed culture system and the hiPS-CM sheets may provide a basis for the clinical use of hiPS cells in cardiac regeneration therapy. **(*Circulation*. 2012;126[suppl 1]:S29–S37.)**

Key Words: pluripotent stem cell ■ regeneration therapy ■ transplantation

The myocardium has limited regenerative capacity, and loss of myocardium due to myocardial infarction therefore leads to heart failure. Despite remarkable recent progress in medical and surgical treatments for heart failure, end-stage heart failure remains a leading cause of morbidity and mortality.[1] Therefore, the myocardium is one of the most important targets in regenerative medicine. Cell therapy has been introduced as a new treatment for heart failure. Clinical trials using bone marrow cells and myoblasts are underway; although these cells improve cardiac performance, chiefly through paracrine cytokine effects, they show limited differentiation into cardiomyocytes.[2]

Induced pluripotent stem (iPS) cells were first generated by nuclear reprogramming of mouse fibroblasts in 2006,[3] and human iPS (hiPS) cells were established in 2007 by the transduction of defined factors.[4,5] The production of hiPS cells poses fewer legal and ethical issues than does the generation of human embryonic stem (ES) cells. In addition, recent studies have demonstrated methods for the highly efficient production from hiPS cells of cardiomyocytes with typical electrophysiological function and pharmacological responsiveness.[6,7] Human iPS cells represent an unlimited source of cardiomyocytes because of their great potential for differentiation and are therefore one of the most promising sources of cells for cardiac regenerative therapy.[8,9] Nevertheless, many important problems, especially the large-scale preparation of cardiomyocytes by differentiation of iPS cells and the elimination of undifferentiated iPS cells to avoid teratoma formation, must be addressed before hiPS cells can be used clinically.[8,9]

The recently developed scaffoldless tissue engineering technique of cell-sheet engineering is applicable to myocar-

From the Department of Cardiovascular Surgery, Osaka University Graduate School of Medicine, Suita, Osaka, Japan (M.K., S.M., K.M., S.F., T.H., T. Kawamura, T. Kuratani, Y.S.); the Medical Center for Translational Research, Osaka University Hospital, Suita, Osaka, Japan (A.S.); the Department of Biostatistics, Hyogo College of Medicine, Nishinomiya, Hyogo, Japan (T.D.); and the Institute of Advanced Biomedical Engineering and Science, TWIns, Tokyo Women's, Medical University, Shinjuku-ku, Tokyo, Japan (T.S., T.O.).

Presented at the 2011 American Heart Association meeting in Orlando, FL, November 13–17, 2011.

The online-only Data Supplement is available at http://circ.ahajournals.org/lookup/suppl/doi:10.1161/CIRCULATIONAHA.111.084343/-/DC1.

Correspondence to Yoshiki Sawa, MD, PhD, 2-2 Yamada-oka, Suita, Osaka, 565-0871, Japan. E-mail sawa-p@surg1.med.osaka-u.ac.jp

Circulation **is available at http://circ.ahajournals.org** **DOI: 10.1161/CIRCULATIONAHA.111.084343**

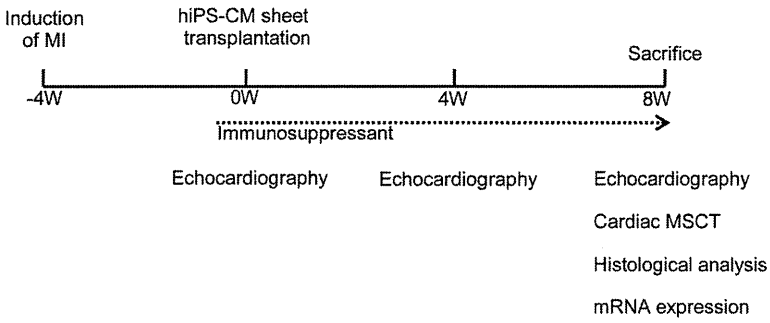

Figure 1. Study protocol of the minipig experiment and the evaluation of cardiac function and histological analysis.

dial regeneration therapy.[10] In contrast to the needle injection technique, the cell-sheet technique can deliver a large number of cells to damaged myocardium without the loss of transplanted cells or injury to the host myocardium. We have previously reported that use of the cell-sheet technique with autologous skeletal myoblasts improves cardiac function in small and large animal models of ischemic cardiomyopathy.[11,12]

We hypothesized that hiPS-derived cardiomyocyte (hiPS-CM)-sheet transplantation would be therapeutically effective in the context of ischemic cardiomyopathy. In this study, we examined the following aspects of this procedure: stable in vitro culture of a large number of cardiomyocytes by differentiation of hiPS cells, generation of hiPS-CM sheets for clinical applications using temperature-responsive dishes, survival of hiPS-CM sheets in the myocardium of a large animal, and the direct contribution of these sheets to the improvement of cardiac performance by structural and electromechanical integration into the recipient myocardium, without teratoma formation, in a porcine ischemic cardiomyopathy model.

Materials and Methods

Animal care complied with the "Guide for the Care and Use of Laboratory Animals" (National Institutes of Health publication No. 85-23, revised 1996). Experimental protocols were approved by the Ethics Review Committee for Animal Experimentation of Osaka University Graduate School of Medicine.

Culture, Differentiation, and Purification of hiPS Cells and Collection of Conditioned Medium

The hiPS cell line 201B7 that was generated using the 4 transcription factors Oct4, Sox2, Klf4, and c-Myc (a generous gift from Professor Yamanaka, Kyoto University, Kyoto, Japan) was used in this study.[4] The hiPS cells were cultured on Matrigel (BD Bioscience)-coated dishes in mTeSR1 medium (Stem Cell Technologies).

Human iPS cells were then dissociated using StemPro Accutase Cell Dissociation Reagent (Invitrogen), transferred to Corning ultralow-attachment surface culture dishes (Sigma-Aldrich) at a density of 50 000 cells/mL in mTeSR1 with Y-27632 (Wako), and cultured for 4 days to allow them to form embryoid bodies. The embryoid bodies were replated with differentiation medium (DMEM-F12; Invitrogen) containing 20% fetal bovine serum, 100 μmol/L nonessential amino acids (Invitrogen), 50 U/mL penicillin, 50 mg/mL streptomycin (Invitrogen), and 5.5 mmol/L 2-mercaptoethanol (Invitrogen) and supplemented with 100 ng/mL Wnt3a (R&D Systems) and 100 ng/mL R-Spondin-1 (Stem RD) and cultured for 2 days. The culture medium was then replaced with differentiation medium without the supplemental factors for 2 days and then changed to differentiation medium supplemented with 100 ng/mL Dkk1 (R&D Systems) for 2 days. On Day 10, the embryoid bodies were plated on gelatin-coated dishes in differentiation medium, which was refreshed every 2 days.

The culture medium was subsequently replaced with no-glucose Dulbecco modified Eagle medium (Invitrogen) with 1 mmol/L lactic acid (Wako; F. Hattori and K. Fukuda. WO2007/088874; PCT/JP2007/051563, 2007) on Day 20 and changed to Dulbecco modified Eagle medium/10% fetal bovine serum the next day. On Day 25, the culture medium was again replaced with no-glucose Dulbecco modified Eagle medium with 1 mmol/L lactic acid and changed to Dulbecco modified Eagle medium/10% fetal bovine serum the next day; this procedure eventually generated pure hiPS-CM. The hiPS-CMs were then labeled with a red fluorescent marker (CellTracker Red CMTPX; Invitrogen) as previously described.[13]

Fetal bovine serum-free Dulbecco modified Eagle medium media were conditioned by hiPS-CMs for 48 hours after the completion of our differentiation and purification protocols. A total of 48 cytokines and growth factors were measured by the Bio-Plex human cytokine assay (Bio-Rad) for in vitro screening.

Preparation of hiPS Cell-Derived Cardiomyocyte Sheets

The hiPS-CMs were detached using StemPro Accutase Cell Dissociation Reagent and seeded onto 6-cm UpCell dishes (CellSeed). The next day, the dish was incubated at room temperature, which caused the cells to detach spontaneously to form scaffold-free hiPS-CM sheets.

Generation of the Porcine Chronic Myocardial Infarction Model and hiPS-CM Sheet Transplantation

A chronic myocardial infarction model was generated by placement of an ameroid constrictor (COR-2.50-SS; Research Instruments) around the left anterior descending coronary artery in female minipigs (Japan Farm) weighing 20 to 25 kg[14] (Figure 1). Four weeks after myocardial infarction induction, transplantation of hiPS-CM sheets was performed through median sternotomy under general anesthesia. All animals were immunosuppressed with daily intake of tacrolimus (0.6 mg/kg; Astellas) from 5 days before transplantation until euthanasia. The minipigs were randomly divided into 2 treatment groups, either hiPS-CM sheet transplantation (iPS group) or sham operation (n=6 each).

Standard and 2-Dimensional Speckle-Tracking Echocardiography

Transthoracic echocardiography was performed under general anesthesia using a 5.0-MHz transducer (Aplio Artida). The left ventricular (LV) end-diastolic and end-systolic diameters were measured, whereas the LV end-diastolic and end-systolic volumes (LVEDV and LVESV, respectively) were calculated from the Teichholz formula.[15] The LV ejection fraction (LVEF) was calculated from the following formula: LVEF (%)=100×(LVEDV−LVESV)/(LVEDV).

Two-dimensional speckle-tracking echocardiography analysis was performed using the customized 2-dimensional speckle-tracking echocardiography software for the Toshiba system (2D Wall Motion Tracking). Regional cardiac function was evaluated using radial strain values obtained from the midshort-axis plane and expressed as a percentage.

Cardiac CT Scan

Electrocardiography-gated multislice CT was performed in the supine position with a 16-slice multislice CT scanner (Somatron Emotion 16; Siemens) during end-expiratory breathhold under general anesthesia. Multislice CT was performed after intravenous injection of 90 mL of nonionic contrast medium (Iomeprol; Bracco Imaging). Axial images were reconstructed using the scanner software. All images were analyzed on a workstation (AZE; Virtual Pl Lexus 64). LVEDV and LVESV were obtained from the workstation and LVEF was calculated using the formula described previously.

Holter Electrocardiography

Holter electrocardiography was performed for 24 hours in both groups (n=6 each). The arrhythmogenesis associated with hiPS-CM sheet transplantation was evaluated based on the number of premature ventricular contractions.

Histology, Immunohistolabeling, and Fluorescence In Situ Hybridization

Dissociated cultured cells were fixed in 4% paraformaldehyde. Primary antibodies included anticardiac troponin T (cTNT; Abcam), anti-Nkx2.5 (Santa Cruz Biotechnology), anti-α-actinin (Sigma-Aldrich), antihuman CD31 (BD Bioscience), antihuman CD34 (BD Bioscience) and antivimentin (BD Bioscience) visualized by fluorescent-conjugated secondary antibodies such as AlexaFluor488 goat antirabbit IgG, AlexaFluor488 goat antimouse IgG, and AlexaFluor488 donkey antigoat IgG (Invitrogen) with counterstaining by 4′6-diamidino-2-phenylindole (Dojindo) and assessed by fluorescence microscopy. Images of the samples were acquired with a Biorevo BZ-9000 (Keyence). Positivity of the cardiomyocyte-specific markers or other lineage markers in the cultured cells was determined from the acquired images by using computer-based cell counting with the Dynamic Cell Count BZ-H1CE software (Keyence).

The excised heart specimen was fixed with either 10% buffered formalin or 4% paraformaldehyde for frozen sections. Picrosirius red or periodic acid-Schiff stains were used to assess interstitial fibrosis or cardiomyocyte hypertrophy, respectively. To evaluate neovascularization in the peri-infarct area, immunolabeling with antihuman von Willebrand factor antibody (Dako) was done. The frozen sections were immunolabeled by the primary antibodies such as anticTNT (Abcam) and antislow myosin heavy chain (Sigma-Aldrich) antibodies, visualized by AlexaFluor488 goat antimouse IgG (Invitrogen), counterstained by 4′,6-diamidino-2-phenylindole, and assessed by fluorescence microscopy or confocal laser microscopy.

The hiPS-CMs at 8 weeks after transplantation were detected by fluorescent in situ hybridization using a human specific genomic probe labeled by Cy3 (Chromosome Science Labs). The samples were double-stained with other antibodies described previously and counterstained with 4′,6-diamidino-2-phenylindole.

Real-Time Polymerase Chain Reaction

Total RNA was extracted from cardiac tissue and reverse transcribed using TaqMan reverse transcription reagents (Applied Biosystems), and real-time polymerase chain reaction was performed with the ABI PRISM 7700 (Applied Biosystems) system using pig-specific primers for vascular endothelial growth factor and basic fibroblast growth factor. The average copy number of gene transcripts was normalized to that of glyceraldehyde-3-phosphate dehydrogenase for each sample.

Statistical Analysis

JMP software (JMP7.01; SAS Institute Inc) was used for all statistical analyses. Continuous values are expressed as the mean±SD. Within-group differences were compared with the Wilcoxon signed-rank test and between-group differences with the Wilcoxon-Mann-Whitney U test because the sample sizes are too small (just n=6 in each group and n=6 pairs) to allow checking of the assumptions of the unpaired and paired *t* tests, respectively. A probability value <0.05 was considered statistically significant.

Results

Generation of Highly Purified hiPS-CM Sheets

Cardiomyogenic differentiation of hiPS cells was induced by treatment of the embryoid bodies formed from cultured hiPS cells with Wnt3a and R-Spondin-1. Subsequently, the differentiated hiPS cells were purified by culture in glucose-free medium to yield hiPS-CMs. The hiPS-CMs were highly positive for the cardiomyocyte-specific markers α-actinin (89.7%±3.8%), cTNT (87.4%±4.2%), and Nkx2.5 (84.2%± 4.3%), as assessed by immunohistolabeling (Figure 2A–D). In addition, the hiPS-CMs included a small population of cells expressing vascular endothelial or endothelial progenitor cell-specific markers such as CD31 (2.9%±3.0%) and CD34 (1.6%±1.4%; Figures 2A, 2E, and 2F). These cells also included a small population of vimentin-positive cells (2.4%±1.0%), which is a marker of fibroblast or smooth muscle cells (Figures 2A and 2G).

Serum-free conditioned media from hiPS-CMs were screened for the secreted factors by using enzyme-linked immunosorbent assay (Figure 2H–I). The media contained high concentrations of various factors such as hepatocyte growth factor (HGF), stromal cell-derived factor (SDF), interluekin 6, leukemia inhibitory factor (LIF), macrophage migration inhibitory factor (MIF), and monocyte chemoattractant protein-1.

Subsequently, culture in the thermoresponsive dishes yielded round-shaped scaffold-free hiPS-CM sheets (Figure 2J). Hematoxylin & eosin-stained cross-sections of the sheet showed a 30- to 50-μm-thick regular structure with abundant extracellular matrix (Figure 2K). Immunohistolabeling showed that the cytoplasm of most of the cells in the hiPS-CM sheets was homogeneously positive for cTNT (Figure 2L).

Feasibility and Safety of hiPS-CM Sheet Transplantation Into the Chronic Myocardial Infarction Heart

Transplantation of 8 hiPS-CM sheets was successfully performed through median sternotomy under general anesthesia in 6 immunosuppressed minipigs with LVEF values of 35% to 45% due to induced chronic myocardial infarction. There was no mortality related to the procedure or otherwise before the planned euthanasia. Twenty-four-hour electrocardiography monitoring only rarely identified ventricular arrhythmias in either group before the planned euthanasia (data not shown). In addition, no teratomas were formed in the heart or other thoracic organs within the 8 weeks after the transplantation of the hiPS-CM sheets (data not shown).

Global Cardiac Functional Recovery After hiPS-CM-Sheet Transplantation

Serial standard transthoracic echocardiography was performed before and 4 and 8 weeks after the cell-sheet transplantation or sham surgery. The baseline LV end-diastolic diameter, LV end-systolic diameter, and LVEF did not differ significantly between the 2 groups. The sham-operated pigs showed nonsignificant upward trends in LV end-diastolic diameter and LV end-systolic diameter and a downward trend in LVEF between 4 and 8 weeks after surgery (Figure 3A–C). LVEF was significantly greater in the iPS group than in the sham group after 4 (53.2%±4.3% versus 38.3%±4.3%, $P<0.01$) and 8 (51.6%±4.9% versus 36.0%±5.9%, $P<0.01$) weeks. LV

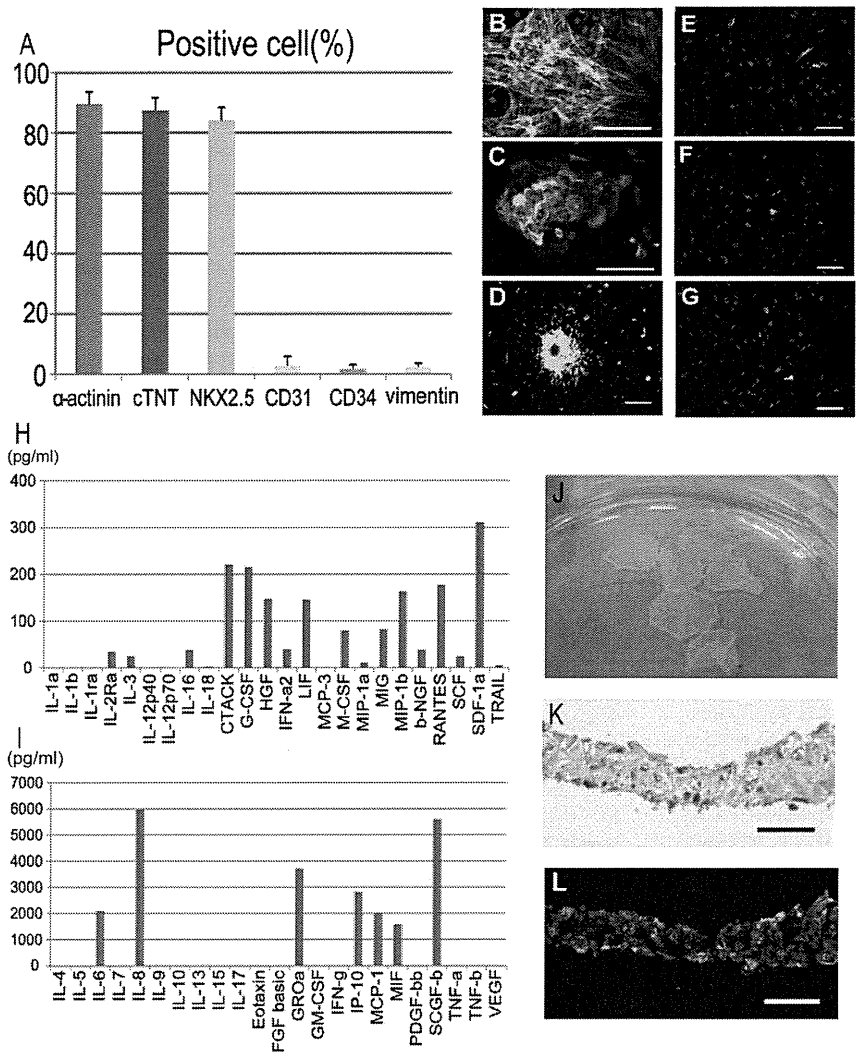

Figure 2. Histological characteristics of the hiPS-CM sheets. **A**, quantitative analysis of the numbers of hiPS-derived cells expressing α-actinin, cTNT, Nkx2.5, CD31, CD34, or vimentin, shown as percentages (%). Almost 90% pure cardiomyocytes were obtained. **B–G**, Immunostaining of the hiPS-CMs with anti-α-actinin (**B**), anticTNT (**C**), and anti-Nkx2.5 (**D**), anti-CD31 (**E**), anti-CD34 (**F**), and antivimentin (**G**) antibodies in green; bar=100 μm in **B–G. H–I**, In vitro screening for cytokines and growth factors. Several factors that may potentially be involved in cardiac repair were detected at relatively high concentrations in the medium. **J**, hiPS-CM sheets in a 10-cm dish. **K–L**, Hematoxylin and eosin (HE) staining (**K**) and immunostaining with cTNT antibody (**L**) of the hiPS-CM sheets in green. Many cTNT-positive cells were detected in the hiPS-CM sheets; bar=50 μm in **K–L**. The cell nuclei were counterstained with 4′,6-diamidino-2-phenylindole (DAPI) in blue (**B, C, E, F, G, L**). hiPS-CM indicates human induced pluripotent stem cell-derived cardiomyocyte.

end-systolic diameter was significantly smaller in the iPS group than in the sham group after 4 (25.0±1.9 mm versus 30.1±3.4 mm, $P<0.05$) and 8 (26.2±3.3 mm versus 34.7±5.4 mm, $P<0.05$) weeks, whereas LV end-diastolic diameter did not differ significantly between the 2 groups.

A cardiac multislice CT scan was performed 8 weeks after the treatment and also demonstrated that LVEF was significantly greater in the iPS group (50.7%±5.4%) than in the sham group (40.5%±1.7%, $P<0.05$; Figure 4A). LVEDV and LVESV were significantly smaller in the iPS group than in the sham group (57.1±7.5 mL versus 76.1±4.1 mL, $P<0.05$, and 28.3±6.0 mL versus 45.3±3.0 mL, $P<0.05$, respectively; Figure 4B–C).

Recovery of Regional LV Wall Motion After hiPS-CM Sheet Transplantation

Serial speckle-tracking echocardiography was performed to compare the strain values at baseline and 4 weeks after the treatment. Radial strain was measured from the midshort-axis plane to evaluate regional wall motion (Figure 5B–C). In the sham group, the radial strain levels in the infarct, the border, and the remote area had not changed significantly after 4 weeks relative to the baseline values. In contrast, in the iPS group, the radial strain in the border area was significantly greater after 4 weeks than at baseline (10.35%±4.17% versus 15.22%±1.66%, $P<0.05$), whereas the radial strain levels in the infarct and the remote area had not changed significantly.

Pathological Hypertrophy, Interstitial Fibrosis, and Vascular Density

The pathological cardiomyocyte hypertrophy, interstitial fibrosis, and vascular density 8 weeks after the treatment were assessed semiquantitatively by periodic acid-Schiff staining, picrosirius red staining, and immunohistochemistry for von Willebrand factor, respectively (Figure 6). The diameters of the cardiomyocytes in the remote area were significantly smaller in the iPS group than in the sham group. There was consistently significantly less accumulation of interstitial fibrosis in the remote area in the iPS group than in the sham group. In addition, the vascular density in the border area was significantly greater in the iPS group than in the sham group.

Upregulation of Vascular Endothelial Growth Factor and Basic Fibroblast Growth Factor Expression in the Border Area After Treatment

The expression levels of growth factors that are expressed in the myocardium and are potentially related to neovascular-

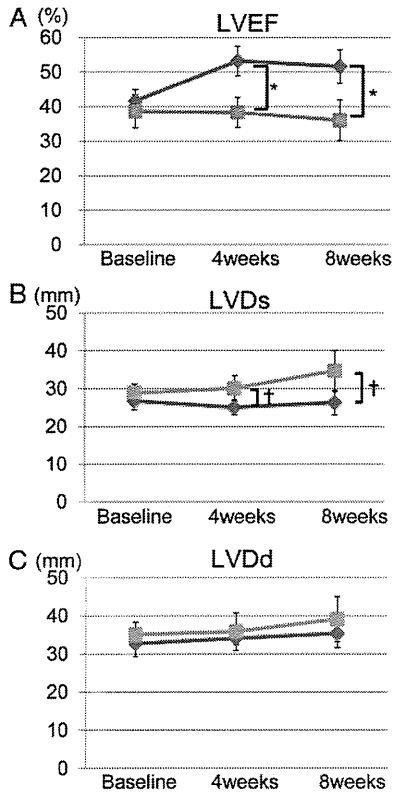

Figure 3. Echocardiographic evaluation. **A**, The global cardiac function as assessed by left ventricular ejection fraction (LVEF) was significantly better in the iPS group. **B**, The left ventricular end-systolic diameter (LVDs) was significantly smaller in the iPS group than in the sham group. **C**, The left ventricular end-diastolic diameter (LVDd) did not differ significantly between the iPS and sham groups. *$P<0.01$, †$P<0.05$ versus sham. The red line indicates the iPS group and the blue line the sham group. iPS indicates induced pluripotent stem cells.

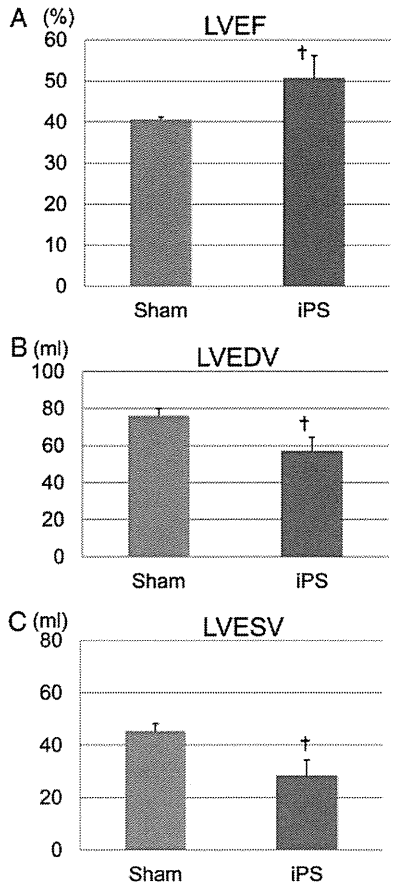

Figure 4. Cardiac multislice CT analysis. **A**, The global cardiac function as assessed by LVEF was significantly better in the iPS group. **B–C**, The left ventricular end-diastolic (LVEDV; **B**) and end-systolic (LVESV; **C**) volumes were significantly smaller in the iPS group than in the sham group. †$P<0.05$ versus sham. LVEF indicates left ventricular ejection fraction; iPS, induced pluripotent stem cells.

ization were quantified by real-time polymerase chain reaction 8 weeks after the treatment. The expression levels of vascular endothelial growth factor and basic fibroblast growth factor in the border area were significantly greater in the iPS group than in the sham group (Figure 7).

Phenotypic Fate of the Transplanted iPS-CMs in the Heart

The hiPS-CMs were labeled in vitro with a red fluorescent marker before transplantation. The labeled cells were identified on the surface of the heart 2 weeks after transplantation. Some of these cells were positive for slow myosin heavy chain (Figure 8A–D). Because the labeled cells could no longer be identified by 8 weeks after transplantation, the presence of the transplanted cells was assessed by fluorescence in situ hybridization using a human-specific genomic probe 8 weeks after transplantation. A small number of human genome-positive cells that expressed slow myosin heavy chain remained present in the infarct area (Figure 8E–G).

Discussion

The major findings of this study were as follows: (1) the newly developed culture system for hiPS cells successfully yielded approximately 2.5×10^7 highly pure hiPS-CMs, and hiPS-CM sheets could be made from these high pure hiPS-CMs using temperature-responsive dishes; (2) the hiPS-CM sheets survived in damaged myocardium in the short term and improved cardiac function in a porcine ischemic cardiomyopathy model, chiefly through the paracrine effects of cytokines. Histological analysis indicated that transplantation of hiPS sheets attenuated left ventricular remodeling and increased neovascularization; and (3) hiPS-derived cardiomyocytes could still be detected 8 weeks after transplantation, but the number of hiPS-CMs that survived long term was very small. No teratoma formation was observed in animals that received hiPS-CM sheets.

The optimal number of cells for clinical use of cardiac regeneration therapy remains unknown. Implantation of approximately 10^8 to 10^9 cells was shown to produce cardiac improvement in previous clinical trials using bone marrow-derived cells.[16] Given these results, it may be necessary to transplant almost this number of hiPS-CMs into impaired myocardium to improve cardiac function in a clinical setting. It is challenging to obtain large numbers of hiPS-CMs at high purity because clinical application of hiPS cells requires 3 steps (ie, proliferation, differentiation, and purification). In

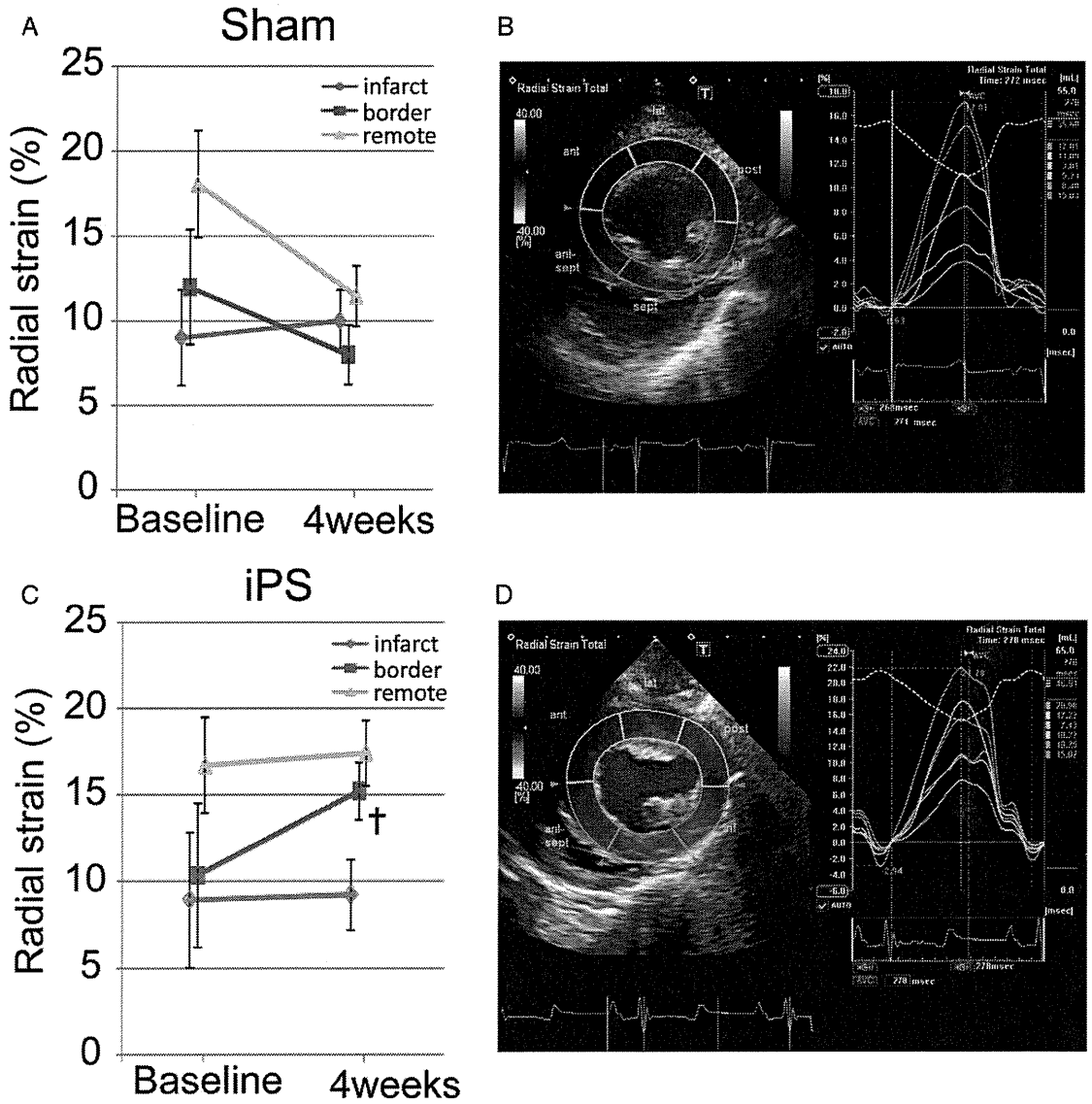

Figure 5. Evaluation of regional wall motion by 2-dimensional speckle-tracking echocardiography. Representative examples of radial strain analysis in each group are shown in **B** (sham) and **D** (iPS). **A**, In the sham group, the radial strain values of all areas did not differ significantly between the baseline and 4 weeks after the sham operation. **C**, In the iPS group, the radial strain value of the border area of the infarct was significantly greater 4 weeks after treatment than at baseline. The radial strain values of the other areas relative to the infarct did not differ significantly before and after hiPS-CM-sheet transplantation. †$P<0.05$ versus baseline. iPS indicates induced pluripotent stem cells; hiPS-CM, human induced pluripotent stem cell-derived cardiomyocyte.

the present study, we obtained approximately 2.5×10^7 hiPS-CMs after differentiation and purification of hiPS cells. One advantage of our culture system for hiPS cells its simplicity, because it involves only supplementation with cytokines for differentiation and culture in glucose-free medium for purification. Our culture system might be able to yield higher numbers of hiPS-CMs and could, possibly, be expanded to a clinically useful scale. Moreover, a previous study evaluating the propensity of secondary neurospheres generated from iPS cells to form teratomas found a significant correlation between the teratoma diameter and the proportion of undifferentiated cells in the secondary neurospheres.[17] Importantly, no teratoma formation was detected in the current experiment, which could be because our purification method limited the number of undifferentiated iPS cells in the hiPS-CMs.

Structural connection and electromechanical integration have been considered to be the mechanisms of functional recovery of the impaired myocardium after ES cell-derived cardiomyocyte transplantation.[18,19] We therefore predicted that the hiPS-CMs would connect structurally and electromechanically with the host myocardium, as seen for ES cell-derived cardiomyocytes. However, although functional cardiac recovery was observed after hiPS-CM-sheet transplantation, only a few transplanted cells were persistently present. It has been shown that the therapeutic effects of stem cell therapy can result from paracrine or direct effects. Paracrine effects have been considered as the major mechanisms responsible for the therapeutic efficacy of cell therapy with somatic tissue-derived stem or progenitor cells. These effects classically refer to the ability of transplanted cells to extracellularly

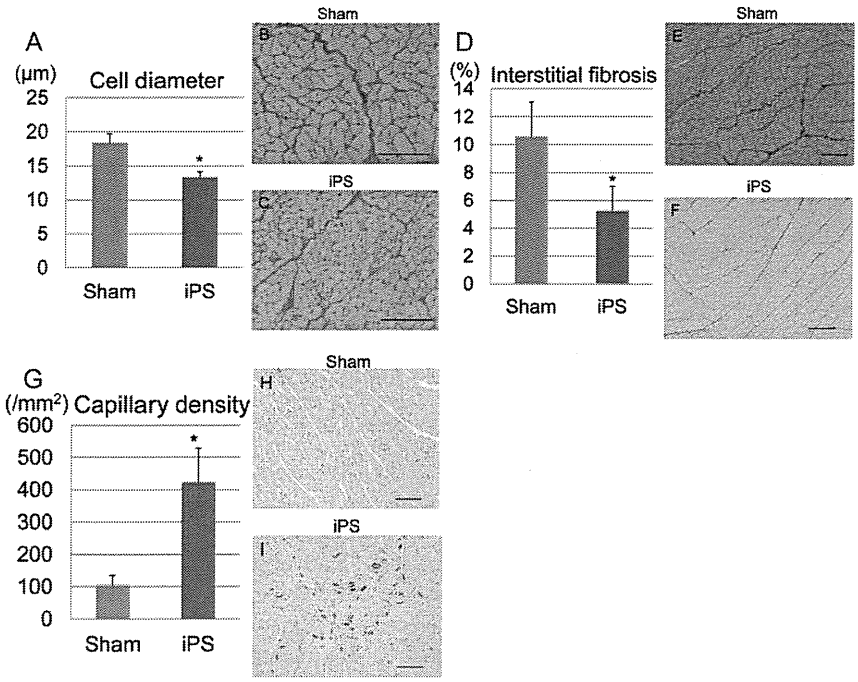

Figure 6. Histological evaluation after hiPS-CM-sheet transplantation. **A–C**, The diameters of the cardiomyocytes were measured at an area remote from the infarct; cardiomyocyte hypertrophy was significantly lower in the iPS group than in the sham group (**A**). Photomicrographs of periodic acid-Schiff (PAS)-stained sections are shown in **B–C**. **D–F**, The proportions of fibrosis-occupied area (%) at a site remote from the infarct; Picrosirius red staining demonstrated significantly less interstitial fibrosis in the iPS group than in the sham group (**D**). Photomicrographs of the Picrosirius red-stained sections are shown in **E–F**. **G–I**, Capillary density in an area bordering the infarct; the capillary density as assessed by immunostaining with an anti-von Willebrand factor antibody was significantly better in the iPS group (**G**). Photomicrographs of immunostaining for von Willebrand factor are shown in **H–I**. *$P<0.01$ versus sham. Bar=100 μm. hiPS-CM indicates human induced pluripotent stem cell-derived cardiomyocyte; iPS, induced pluripotent stem cells.

release various cardioprotective factors into the damaged cardiac tissue to directly enhance reverse LV remodeling. In contrast, recent reports have suggested that cell transplantation upregulates various cardioprotective factors native to the cardiac tissue through "crosstalk" between the transplanted cells and the native cardiac tissue.[2,20] In addition, another report has shown that paracrine effects of human cardiosphere-derived cells, which are capable of directed cardiac regeneration in vivo, play important roles in improving infarcted myocardium.[21] In our study, we observed that several factors, which were reportedly involved in cardiac repair,[20] were secreted by hiPS-CMs during in vitro screening. Consequently, cardiomyocyte hypertrophy and interstitial fibrosis were significantly attenuated in the infarct-remote area after cell sheet transplantation. In addition, capillary density was increased in the infarct border area associated with the upregulation of vascular endothelial growth factor and basic fibroblast growth factor after cell sheet transplantation. Speckle-tracking echocardiography showed that the regional function in the corresponding area was preserved after cell sheet transplantation as compared with that after a sham operation, in which the regional function progressively deteriorated. This suggests that ischemia-related hibernation in the infarct border myocardium might have recovered by increased blood flow because of angiogenesis. These findings suggest that in our study, paracrine effects are the major mechanisms underlying the functional improvement after hiPS-CM-sheet implantation. In contrast, only a small fraction of the transplanted cells differentiated into cardiac lineage, as assessed by fluorescence in situ hybridization analysis, which clearly distinguished cells of human origin from porcine cardiac tissue. This finding suggests that direct effects were not a major contributing mechanism responsible for the functional benefits observed in this study. Therefore,

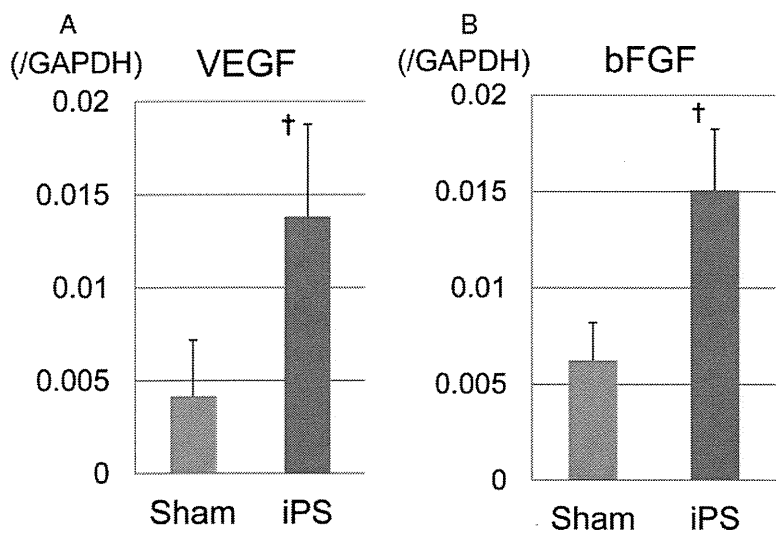

Figure 7. Neovascularization-related mRNA expression in an area bordering the infarct measured by real-time polymerase chain reaction (RT-PCR). The mRNA expression levels of vascular endothelial growth factor (VEGF; **A**) and basic fibroblast growth factor (bFGF; **B**) were significantly higher in the iPS group than in the sham group. †$P<0.05$ versus sham. iPS indicates induced pluripotent stem cells.

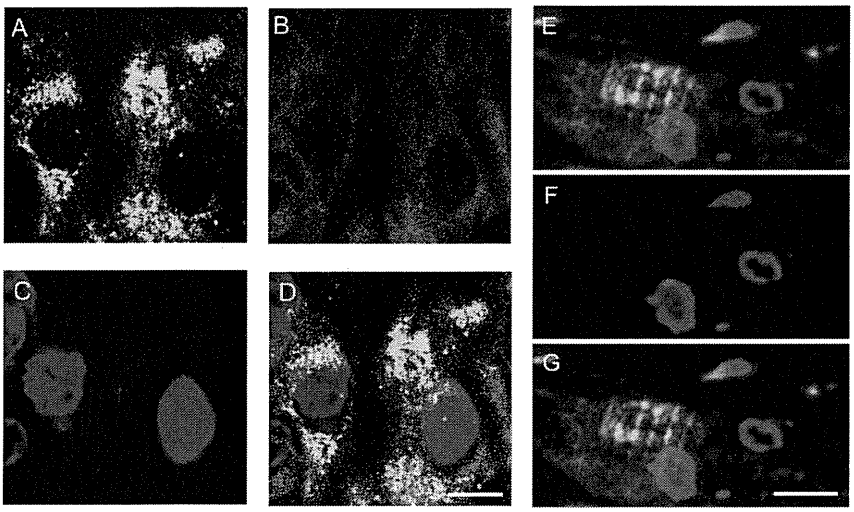

Figure 8. The hiPS-CMs in the heart after transplantation. **A–D**, Detection of red fluorescence-labeled hiPS-CMs 2 weeks after transplantation; representative photomicrographs showing slow myosin heavy chain (sMHC) in green (**A**) and labeled hiPS-CMs in red (**B**). **E–G**, Detection of hiPS-CMs 8 weeks after transplantation by fluorescence in situ hybridization (FISH) using a human-specific genomic probe; immunostaining for sMHC is shown in green (**E**) and positive FISH signals in red (**F**). The nuclei were stained with DAPI in blue (**C, E, F**). Merged images are shown in **D** and **G**. Bar=10 μm in **D** and **G**. hiPS-CM indicates human induced pluripotent stem cell-derived cardiomyocyte; DAPI, 4′,6-diamidino-2-phenylindole dihydrochloride.

it will be important to develop additive treatment to enhance survival, differentiation, and integration of the transplanted cells into the cardiac tissue.

Histological analysis revealed that most of the implanted hiPS-CMs disappeared after implantation, indicating poor engraftment of the hiPS-CMs into the impaired myocardium. In our study, hiPS-CMs secreted multiple angiogenic factors or their inducers, and the hiPS-CMs included small populations of CD31- or CD34-positive cells. These findings indicate that the hiPS-CM sheets have angiogenic potential, which might result in the generation of new vascular networks between the hiPS-CM sheets and the host cardiac tissue. A previous report has shown that the prompt formation of a vascular network between the cell sheet and the surrounding host tissue can sufficiently supply blood and oxygen to the transplanted cell sheet to survive and function in the host tissue.[22] However, in the present study, the host myocardium persistently experienced low blood supply due to coronary artery occlusion, which can interfere with the formation of a new vascular network between the cardiac tissue and the transplanted hiPS-CM sheets, possibly leading to poor survival and differentiation of the transplanted cells in the heart. Poor engraftment has been shown after experimental transplantation of human ES cell-derived cardiomyocytes through simple injection into the infarcted myocardium; treatment with several factors that block cell death pathways improved the engraftment of transplanted ES cell-derived cardiomyocytes.[23] We recently established a new method of cell protection by gene transfection[24] and a novel cell delivery system using the omentum,[25] which can enhance the therapeutic effects of cell therapy. Additional methods of prolonging cell survival after implantation might be necessary to improve the engraftment rate and thus obtain long-standing therapeutic effects of the hiPS-CM sheet from not only paracrine factors, but also direct contributions to the host heart.

Successful regeneration therapy using human pluripotent stem cells requires that the stem cells or their derivatives remain in the recipient myocardium long term. Unless the cell transplantation is autogeneic, the cells will inevitably be rejected by the immune system. Future clinical applications of hiPS cells for regeneration therapy may involve allogeneic and HLA type-matched transplantations, because some acute injuries such as myocardial infarction, stroke, or spinal cord trauma are targeted for regeneration therapy.[26] Therefore, elimination of immunologic rejection or induction of immunologic tolerance of the transplanted stem cells or their derivatives is a critical issue in stem cell-based medicine.[27] In the present study, we used tacrolimus as the only immunosuppressant in a xenotransplantation model; therefore, the failure of prolonged engraftment of hiPS-CMs could have been due to insufficient immunosuppressive therapy. A previous study has demonstrated that combined therapy with tacrolimus and sirolimus significantly prolonged the survival of human ES cells in a xenotransplantation model.[28] In another experiment, blocking the leukocyte costimulatory molecules was found to promote successful engraftment of ES and iPS cells in allogeneic and xenogeneic transplantation models.[26] These findings indicate that appropriate immunosuppressive therapies could improve stem cell engraftment. However, the immunogenicity of iPS cells has not yet been fully investigated. Further studies are needed to establish appropriate strategies for inducing and maintaining immunologic tolerance during the clinical use of allogeneic iPS cell therapy.

In conclusion, the present study showed that our culture system yields a large number of highly pure hiPS-CMs and that hiPS-CM sheets could improve cardiac function in the context of ischemic cardiomyopathy, primarily through paracrine cytokine effects. This newly developed culture system and the hiPS-CM sheets may provide a basis for clinical hiPS-CM-sheet transplantation as part of a strategy for promoting the regeneration of damaged myocardium.

Acknowledgments

We thank Shigeru Matsumi, Masako Yokoyama, and Akima Harada for excellent technical assistance.

Disclosures

Dr Shimizu is a consultant for CellSeed, Inc. Dr Okano is an Advisory Board Member in CellSeed, Inc, and an inventor/developer designated on the patent for temperature-responsive culture surfaces.

References

1. Jessup M, Brozena S. Heart failure. *N Engl J Med.* 2003;348:2007–2018.
2. Gonzales C, Pedrazzini T. Progenitor cell therapy for heart disease. *Exp Cell Res.* 2009;315:3077–3085.
3. Takahashi K, Yamanaka S. Induction of pluripotent stem cells from mouse embryonic and adult fibroblast cultures by defined factors. *Cell.* 2006;126:663–676.
4. Takahashi K, Tanabe K, Ohnuki M, Narita M, Ichisaka T, Tomoda K, Yamanaka S. Induction of pluripotent stem cells from adult human fibroblasts by defined factors. *Cell.* 2007;131:861–872.
5. Yu J, Vodyanik MA, Smuga-Otto K, Antosiewicz-Bourget J, Frane JL, Tian S, Nie J, Jonsdottir GA, Ruotti V, Stewart R, Slukvin II, Thomson JA. Induced pluripotent stem cell lines derived from human somatic cells. *Science.* 2007;318:1917–1920.
6. Germanguz I, Sedan O, Zeevi-Levin N, Shtrichman R, Barak E, Ziskind A, Eliyahu S, Meiry G, Amit M, Itskovitz-Eldor J, Binah O. Molecular characterization and functional properties of cardiomyocytes derived from human inducible pluripotent stem cells. *J Cell Mol Med.* 2011;15:38–51.
7. Ren Y, Lee MY, Schliffke S, Paavola J, Amos PJ, Ge X, Ye M, Zhu S, Senyei G, Lum L, Ehrlich BE, Qyang Y. Small molecule Wnt inhibitors enhance the efficiency of BMP-4-directed cardiac differentiation of human pluripotent stem cells. *J Mol Cell Cardiol.* 2011;51:280–287.
8. Yamashita JK. ES and iPS cell research for cardiovascular regeneration. *Exp Cell Res.* 2010;316:2555–2559.
9. Yoshida Y, Yamanaka S. iPS cells: a source of cardiac regeneration. *J Mol Cell Cardiol.* 2011;50:327–332.
10. Masuda S, Shimizu T, Yamato M, Okano T. Cell sheet engineering for heart tissue repair. *Adv Drug Deliv Rev.* 2008;60:277–285.
11. Memon IA, Sawa Y, Fukushima N, Matsumiya G, Miyagawa S, Taketani S, Sakakida SK, Kondoh H, Aleshin AN, Shimizu T, Okano T, Matsuda H. Repair of impaired myocardium by means of implantation of engineered autologous myoblast sheets. *J Thorac Cardiovasc Surg.* 2009;130:646–653.
12. Miyagawa S, Saito A, Sakaguchi T, Yoshikawa Y, Yamauchi T, Imanishi Y, Kawaguchi N, Teramoto N, Matsuura N, Iida H, Shimizu T, Okano T, Sawa Y. Impaired myocardium regeneration with skeletal cell sheets. A preclinical trial for tissue-engineered regeneration therapy. *Transplantation.* 2010;90:364–372.
13. Jaroszeski MJ, Gilbert R, Heller R. Detection and quantitation of cell–cell electrofusion products by flow cytometry. *Anal Biochem.* 1994;216:271–275.
14. Teramoto N, Koshino K, Yokoyama I, Miyagawa S, Zeniya T, Hirano Y, Fukuda H, Enmi J, Sawa Y, Knuuti J, Iida H. Experimental pig model of old myocardial infarction with long survival leading to chronic left ventricular dysfunction and remodeling as evaluated by PET. *J Nucl Med.* 2011;52:761–768.
15. Teichholz LE, Kreulen T, Herman MV, Gorlin R. Problems in echocardiographic volume determinations: echocardiographic–angiographic correlations in the presence or absence of asynergy. *Am J Cardiol.* 1976;37:7–11.
16. Rosenzweig A. Cardiac cell therapy—mixed results from mixed cells. *N Engl J Med.* 2006;355:1274–1277.
17. Miura K, Okada Y, Aoi T, Okada A, Takahashi K, Okita K, Nakagawa M, Koyanagi M, Tanabe K, Ohnuki M, Ogawa D, Ikeda E, Okano H, Yamanaka S. Variation in the safety of induced pluripotent stem cell lines. *Nat Biotechnol.* 2009;27:743–745.
18. Caspi O, Huber I, Kehat I, Habib M, Arbel G, Gepstein A, Yankelson L, Aronson D, Beyar R, Gepstein L. Transplantation of human embryonic stem cell-derived cardiomyocytes improves myocardial performance in infarcted rat hearts. *J Am Coll Cardiol.* 2007;50:1884–1893.
19. Kehat I, Khimovich L, Caspi O, Gepstein A, Shofti R, Arbel G, Huber I, Satin J, Itskovitz-Eldor J, Gepstein L. Electromechanical integration of cardiomyocytes derived from human embryonic stem cells. *Nat Biotechnol.* 2004;22:1282–1289.
20. Gnecchi M, Zhang Z, Ni A, Dzau VJ. Paracrine mechanisms in adult stem cell signaling and therapy. *Circ Res.* 2008;103:1204–1219.
21. Chimenti I, Smith RR, Li TS, Gerstenblith G, Messina E, Giacomello A, Marbán E. Relative roles of direct regeneration versus paracrine effects of human cardiosphere-derived cells transplanted into infarcted mice. *Circ Res.* 2010;106:971–980.
22. Shimizu T, Sekine H, Yang J, Isoi Y, Yamato M, Kikuchi A, Kobayashi E, Okano T. Polysurgery of cell sheet grafts overcomes diffusion limits to produce thick, vascularized myocardial tissues. *FASEB J.* 2006;20:708–710.
23. Laflamme MA, Chen KY, Naumova AV, Muskheli V, Fugate JA, Dupras SK, Reinecke H, Xu C, Hassanipour M, Police S, O'Sullivan C, Collins L, Chen Y, Minami E, Gill EA, Ueno S, Yuan C, Gold J, Murry CE. Cardiomyocytes derived from human embryonic stem cells in pro-survival factors enhance function of infarcted rat hearts. *Nat Biotechnol.* 2007;25:1015–1024.
24. Miyagawa S, Sawa Y, Taketani S, Kawaguchi N, Nakamura T, Matsuura N, Matsuda H. Myocardial regeneration therapy for heart failure: hepatocyte growth factor enhances the effect of cellular cardiomyoplasty. *Circulation.* 2002;105:2556–2561.
25. Shudo Y, Miyagawa S, Fukushima S, Saito A, Shimizu T, Okano T, Sawa Y. Novel regenerative therapy using cell-sheet covered with omentum flap delivers a huge number of cells in a porcine myocardial infarction model. *J Thorac Cardiovasc Surg.* 2011;142:1188–1196.
26. Pearl JI, Lee AS, Leveson-Gower DB, Sun N, Ghosh Z, Lan F, Ransohoff J, Negrin RS, Davis MM, Wu JC. Short-term immunosuppression promotes engraftment of embryonic and induced pluripotent stem cells. *Cell Stem Cell.* 2011;8:309–317.
27. Chidgey AP, Layton D, Trounson A, Boyd RL. Tolerance strategies for stem-cell-based therapies. *Nature.* 2008;453:330–337.
28. Swijnenburg RJ, Schrepfer S, Govaert JA, Cao F, Ransohoff K, Sheikh AY, Haddad M, Connolly AJ, Davis MM, Robbins RC, Wu JC. Immunosuppressive therapy mitigates immunological rejection of human embryonic stem cell xenografts. *Proc Natl Acad Sci U S A.* 2008;105:12991–12996.

Circulation
JOURNAL OF THE AMERICAN HEART ASSOCIATION

American Heart Association®

Mitral Valve Repair for Medically Refractory Functional Mitral Regurgitation in Patients With End-Stage Renal Disease and Advanced Heart Failure

Satoshi Kainuma, Kazuhiro Taniguchi, Takashi Daimon, Taichi Sakaguchi, Toshihiro Funatsu, Shigeru Miyagawa, Haruhiko Kondoh, Koji Takeda, Yasuhiro Shudo, Takafumi Masai, Mitsuru Ohishi and Yoshiki Sawa

Circulation. 2012;126:S205-S213
doi: 10.1161/CIRCULATIONAHA.111.077768
Circulation is published by the American Heart Association, 7272 Greenville Avenue, Dallas, TX 75231

Print ISSN: 0009-7322. Online ISSN: 1524-4539

Mitral Valve Repair for Medically Refractory Functional Mitral Regurgitation in Patients With End-Stage Renal Disease and Advanced Heart Failure

Satoshi Kainuma, MD; Kazuhiro Taniguchi, MD, PhD; Takashi Daimon, PhD; Taichi Sakaguchi, MD, PhD; Toshihiro Funatsu, MD, PhD; Shigeru Miyagawa, MD, PhD; Haruhiko Kondoh, MD, PhD; Koji Takeda, MD, PhD; Yasuhiro Shudo, MD; Takafumi Masai, MD, PhD; Mitsuru Ohishi, MD, PhD; Yoshiki Sawa, MD, PhD

Background—Information regarding patient selection for mitral valve repair for chronic kidney disease or end-stage renal disease (ESRD) with severe heart failure (HF) as well as outcome is limited.

Methods and Results—We classified 208 patients with advanced HF symptoms (Stage C/D) undergoing mitral valve repair for functional mitral regurgitation into 3 groups: estimated glomerular filtration rate ≥30 mL/min/1.73 m^2 (control group, n=144); estimated glomerular filtration rate <30 mL/min/1.73 m^2, not dependent on hemodialysis (late chronic kidney disease group, n=45), and ESRD on hemodialysis (ESRD group, n=19; preoperative hemodialysis duration 83±92 months). Follow-up was completed with a mean duration of 49±25 months. Postoperative (1-month) cardiac catheterization showed that left ventricular end-systolic volume index decreased from 109±38 to 79±41, 103±31 to 81±31, and 123±40 to 76±34 mL/m^2, in the control, late chronic kidney disease, and ESRD groups, respectively. Left ventricular end-diastolic pressure decreased, whereas cardiac index increased in all groups with no intergroup differences for those postoperative values. Freedom from mortality and HF readmission at 5 years was 18%±7% in late chronic kidney disease ($P<0.0001$ versus control, $P=0.01$ versus ESRD), and 64%±12% in ESRD ($P=1$ versus control) as compared with 52%±5% in the control group (median event-free survival, 26, 67, and 63 months, respectively).

Conclusions—Mitral valve repair for medically refractory functional mitral regurgitation in patients with advanced HF yielded improvements in left ventricular function and hemodynamics irrespective of preoperative renal function status. Patients with ESRD showed favorable late outcome in terms of freedom from mortality and readmission for HF as compared with those with late chronic kidney disease. Further studies are needed to assess the survival benefits of mitral valve repair in patients with ESRD and advanced HF. **(*Circulation*. 2012;126[suppl 1]:S205–S213.)**

Key Words: cardiomyopathy ■ chronic kidney disease ■ end-stage renal disease ■ functional mitral regurgitation ■ mitral valve repair

Heart failure and end-stage renal failure (ESRD) requiring dialysis are major health problems in Japan, as in the United States. Heart failure and chronic kidney disease (CKD) share a number of major risk factors, including hypertension and diabetes mellitus, and a substantial proportion of patients with advanced heart failure have impaired renal function.[1] Heart failure is the leading cause of mortality in patients with CKD or ESRD, whereas impaired renal function is strongly associated with poor outcomes in patients with chronic heart failure.[2] Moreover, kidney dysfunction per se is a risk factor for developing left ventricular (LV) remodeling and heart failure.[3,4]

Ischemic or nonischemic dilated cardiomyopathy is frequently complicated by functional mitral regurgitation (MR) as a consequence of LV remodeling progression. Medically refractory severe functional MR has a strong negative impact on survival of patients with CKD or ESRD and advanced heart failure. An increasing number of patients with ESRD has led to increased referrals of patients on dialysis for surgical repair of functional MR and other concomitant procedures.[5]

From the Department of Cardiovascular Surgery, Japan Labor Health and Welfare Organization Osaka Rosai Hospital, Sakai, Osaka, Japan (S.K., Ka.T., T.F., H.K.); the Departments of Cardiovascular Surgery (S.K., T.S., S.M., Ko.T., Ya.S., Yo.S.) and Geriatric Medicine and Nephrology (M.O.), Osaka University Graduate School of Medicine, Suita, Osaka, Japan; the Department of Biostatistics, Hyogo College of Medicine, Nishinomiya, Hyogo, Japan (T.D.); and Osaka Cardiovascular Surgery Research (OSCAR) group, Osaka, Japan (T.M.).

Presented at the 2011 American Heart Association meeting in Orlando, FL, November 13–17, 2011.

The online-only Data Supplement is available at http://circ.ahajournals.org/lookup/suppl/doi:10.1161/CIRCULATIONAHA.111.077768/-/DC1.

Correspondence to Yoshiki Sawa, MD, PhD, Department of Cardiovascular Surgery, Osaka University Graduate School of Medicine, 2-2-E1, Yamadaoka, Suita, Osaka 565-0871, Japan. E-mail Sawa@surg1.med.osaka-u.ac.jp

Circulation **is available at http://circ.ahajournals.org** **DOI: 10.1161/CIRCULATIONAHA.111.077768**

The EuroSCORE II calculator (www.euroscore.org/calc.html) shows that impaired renal function (ie, creatinine clearance <50 mL/min) off dialysis is a major risk factor for postoperative mortality in patients undergoing cardiovascular surgery, and patients with ESRD on dialysis are sometimes considered to be a relative contraindication to surgical intervention for medically refractory functional MR because other risk factors are commonly associated with this condition. Thus, surgical indication and patient selection for repair of functional MR in patients with CKD or ESRD are controversial, and risk stratification is not supported by the online STS Risk Calculator (http://209.220.160.181/STSWebRiskCalc261/de.aspx). Furthermore, long-term outcomes of patients with CKD or ESRD after surgery have not been sufficiently reported.[6]

We investigated the outcomes of patients with ESRD and advanced heart failure who underwent a restrictive mitral annuloplasty and other concomitant procedures for medically refractory severe functional MR.

Patients and Methods

Between August 1999 and July 2010, 226 consecutive patients with advanced cardiomyopathy were referred for surgical treatment of medically refractory severe or moderate-to-severe (regurgitant volume >30 mL/beat) functional MR and concomitant surgical procedures. Patients who underwent an emergency operation or with recent myocardial infarction (<3 months) were excluded; thus, 208 (166 men, 42 women; 65±10 years old) were analyzed in this retrospective study. Functional MR was caused by restrictive leaflet motion secondary to global severe LV dilatation (Type IIIb MR, Carpentier's classification) in all. Patients with organic MR, rheumatic mitral disease, or aortic valve disease were excluded. All had advanced (Stage C/D) heart failure symptoms and severe LV remodeling (ejection fraction [EF] <40%, end-systolic volume index >60 mL/m^2).

Our institutional ethical committees approved this study and written informed consent for the procedures was obtained from each patient before surgery.

Patient Stratification Based on Preoperative Renal Function

Estimated glomerular filtration rate was calculated by the Modification of Diet in Renal Disease equation.[7] Eight patients had an estimated glomerular filtration rate of >90 mL/min/1.73 m^2 (CKD Stage 1), 136 an estimated glomerular filtration rate of 60 to 89 or 30 to 59 mL/min/1.73 m^2 (CKD Stage 2 or 3), and 45 an estimated glomerular filtration rate of 15 to 29 or <15 mL/min/1.73 m^2 (CKD Stage 4 or 5: late CKD group). Nineteen patients had ESRD on hemodialysis (ESRD group), whereas 144 with CKD Stage 1 to 3 served as the control group.

Hemodialysis was introduced due to progression of diabetic nephropathy in 11, glomerular nephritis in 5, glomerular sclerosis in one, and unknown in 2 patients. Maintenance dialysis had been given for an average of 83±92 months (range, 3–300 months) before surgery. Patient characteristics for the 3 groups are presented in Table 1.

Echocardiography

Two-dimensional and Doppler transthoracic echocardiography examinations were performed before and 1 month after surgery, and annually thereafter. Measurements included LV end-diastolic dimension, LV end-systolic dimension, and LVEF. Systolic pulmonary artery pressure (PAP) was calculated by adding the value for right ventricular systolic pressure, derived from tricuspid regurgitation, to estimated right atrial pressure.[8,9] The inferior vena cava (IVC) dimension was measured through a subcostal approach. It was previously reported that IVC dimension is an accurate predictor of

Table 1. Patient Characteristics

Variables	Control (n=144)	Late CKD (n=45)	ESRD on HD (n=19)
Age, y*	64±10	68±9	64±6
Males	119 (83%)	33 (73%)	14 (74%)
Body surface area, m^2	1.65±0.18	1.62±0.17	1.57±0.16
NYHA class			
I	0 (0%)	0 (0%)	0 (0%)
II	13 (9%)	4 (9%)	1 (5%)
III	112 (78%)	32 (71%)	15 (79%)
IV	19 (13%)	9 (20%)	3 (16%)
Etiologies of cardiomyopathy*			
Ischemic cardiomyopathy	103 (72%)	34 (76%)	15 (79%)
Dilated cardiomyopathy	41 (28%)	11 (24%)	2 (11%)
Uremic cardiomyopathy	0 (0%)	0 (0%)	2 (11%)
Duration of preoperative HD			83±92
Comorbidity			
Hypertension	79 (55%)	28 (62%)	8 (42%)
Hyperlipidemia	58 (40%)	18 (40%)	4 (21%)
Diabetes	61 (42%)	24 (53%)	11 (58%)
Chronic obstructive lung disease	11 (8%)	3 (7%)	0 (0%)
Peripheral vascular disease	12 (8%)	5 (11%)	3 (16%)
Cerebral vascular accident	21 (15%)	8 (18%)	4 (21%)
Atrial fibrillation	45 (31%)	12 (27%)	6 (32%)
History of ventricular arrhythmia	26 (18%)	11 (24%)	3 (16%)
Previous cardiac surgery	13 (9%)	4 (9%)	1 (5%)
Previous CABG	9 (6%)	3 (7%)	0 (0%)
Previous PCI	61 (42%)	21 (47%)	4 (21%)
Laboratory examination			
Creatinine, mg/dL*	1.1±0.3	2.2±0.6	7.7±3.1
eGFR, mL/min/1.73 m^2*	57±19	23±5	7±3
Hemoglobin, g/dL*	13.1±2.1	11.3±2.2	10.4±1.4
Brain natriuretic peptide, pg/mL*	643±498	645±284	2335±1432
Medications			
Beta-blockers	96 (67%)	29 (64%)	10 (53%)
ACE inhibitors	46 (32%)	16 (36%)	3 (16%)
Angiotensin II receptor blockers	48 (33%)	13 (29%)	2 (11%)
Diuretics*	116 (81%)	34 (76%)	5 (26%)
Surgical data			
Mitral annuloplasty ring size			
24 mm	69 (48%)	27 (60%)	13 (68%)
26 mm	64 (44%)	17 (38%)	5 (26%)
28 mm	11 (8%)	1 (2%)	1 (6%)
Mitral annuloplasty alone	54 (38%)	21 (47%)	3 (16%)
Mitral annuloplasty+CABG	45 (31%)	12 (27%)	9 (47%)
Mitral annuloplasty+SVR	21 (15%)	6 (13%)	2 (11%)
Mitral annuloplasty+CABG+SVR	24 (17%)	6 (13%)	5 (26%)

Continuous variables are summarized as the mean±SD.

CKD indicates chronic kidney disease; ESRD, end-stage renal disease; HD, hemodialysis; NYHA, New York Heart Association; CABG, coronary artery bypass grafting; PCI, percutaneous coronary intervention; eGFR, estimated glomerular filtration rate; ACE, angiotensin-converting enzyme; SVR, surgical ventricular reconstruction.

*P<0.05 (one-way analysis of variance).

right atrial pressure and useful for monitoring volume status in patients with heart failure.[10]

Cardiac Catheterization

Cardiac catheterization was performed before and 1 month after surgery. Before left ventriculography, LV systolic pressure, end-diastolic pressure, pulmonary capillary wedge pressure, systolic and mean PAP, and right atrial pressure were measured. Using biplane cine-ventriculography, LV end-diastolic volume, LV end-systolic volume, and LVEF were determined. Cardiac output was measured by the thermodilution method. Volumes and cardiac output were indexed by body surface area.

The purposes of cardiac catheterization and its invasive nature were explained in detail to all patients, and only those who gave informed consent underwent catheterizations. The indications for postoperative catheterization were not selective and the procedure was performed by a cardiologist under appropriate hydration conditions. Preoperative coronary arteriography was performed in all 208 patients, whereas serial left ventriculography and hemodynamic measurements were performed in 154 (74%) and 109 (52%), respectively.

Surgical Procedures

All operations were performed with bicaval cannulation, mild hypothermic cardiopulmonary bypass, and meticulous myocardial preservation with intermittent cold blood cardioplegia. Coronary artery bypass grafting was generally performed first. The approach to the mitral valve was generally through a superior transseptal method. The mitral valve was repaired using a restrictive mitral annuloplasty technique with an undersized ring.[11] Ring size was determined after careful intraoperative measurements of the height of the anterior leaflet and intertrigonal distance and then downsizing by 2 to 3 sizes. No other adjunct procedures were performed on the valve itself. Surgical ventricular reconstruction was performed when a broad anteroapical or anteroseptal asynergy (akinesis or dyskinesis) was demonstrated by left ventriculography and a postoperative LV end-diastolic volume index >90 mL/m^2 was anticipated. Our criteria for adding surgical ventricular reconstruction to restrictive mitral annuloplasty were mainly based on 2 previous investigations.[12,13]

Perioperative Management for Patients With Hemodialysis

Hemodialysis was performed in all patients with ESRD 12 to 24 hours before surgical intervention. During surgery, an extracorporeal ultrafiltration method was used to appropriately maintain volume status. Hemodialysis was routinely resumed on the second postoperative day or earlier if volume overload or hyperkalemia was present.

Clinical Follow-Up

Every 6 months to 1 year, each patient was assessed in the department as well as by their primary cardiologist. Functional status was assessed according to New York Heart Association criteria and plasma brain natriuretic peptide (BNP) level. The primary study end point was mortality during follow-up, and the second was defined as the composite of mortality and readmission for heart failure. Diagnosis of postoperative recurrent heart failure was based on clinical symptoms, physical signs, or radiological evidence of pulmonary congestion.

Clinical follow-up examinations were completed for all patients (100%) with a mean duration of 49±25 months (range, 4–126 months) for survivors. The cumulative follow-up period was 728 patient-years.

Statistical Analysis

Continuous variables are summarized as means±SDs or SEs when describing data presented in a figure and categorical variables as frequencies and proportions. For the continuous variables, comparisons between 2 groups were made using an unpaired *t* test. Comparisons among 3 groups were made using one-way analysis of variance. For categorical variables, 3 groups were compared using Fisher exact or a Kruskal-Wallis test. Correlations between continuous variables were tested with Pearson correlation coefficient (*r*). Hemodynamic data (LV end-diastolic volume index, LV end-systolic volume index, LVEF, LV end-diastolic pressure, mean PAP, cardiac index) were analyzed using an analysis of covariance model, including factors for the corresponding baseline value as the covariate, group, and interaction between them. Functional (plasma BNP) and echocardiographic (LV end-diastolic dimension, LV end-systolic dimension, LVEF, systolic PAP) data over time after surgical intervention were analyzed using a mixed-effects model for repeated measures, including factors for the corresponding baseline value, group, time, and interaction between group and time. The following covariance structures were considered: unstructured, compound symmetrical, first-order autoregressive, and Toeplitz. The covariance structure that provided the best fit according to Akaike information criterion was used in the analysis. Assessment time points were treated as categorical factors. The analysis of covariance and mixed-effects models included adjustments for age, etiology of cardiomyopathy, with or without diuretics, and laboratory examination findings, which showed significant differences among the groups (Table 1).

The linearized mortality rate was computed by dividing the number of patients experiencing an event by patient-years at risk. Survival and adverse event-free curves were estimated using the Kaplan-Meier method, and compared using an overall log-rank test, followed by a post hoc pairwise log-rank test. The association of group with adverse events was examined using Cox proportional-hazards models with adjustments for all other covariates presented in baseline demographics, echocardiographic, and surgical data (see the online-only Data Supplement Appendix). Factors obtaining a probability value <0.05 in the univariate Cox proportional hazards analysis were then entered appropriately into the multivariate fashion. Results are summarized as hazard ratios and 95% CIs. Multiplicity in pairwise comparisons was corrected by the Bonferroni procedure. All probability values are 2-sided and values of $P<0.05$ were considered to indicate statistical significance. Statistical analyses were performed using JMP 7.0 (SAS Institute, Cary, NC), SAS statistical software (Version 9.2; SAS Institute), and SPSS (Version 17.0; SPSS Inc).

Results

Clinical Outcomes

Overall hospital mortality was 6.3% for all patients and 6.3%, 6.7%, and 5.3% for the control, late CKD, and ESRD groups, respectively, with no intergroup differences.

Among 195 operative survivors, 49 late deaths occurred during the follow-up period with a linearized mortality rate of 6.8% per patient-year. Patients with ESRD tended to die from infectious or bleeding disorders rather than cardiac causes, whereas those with late CKD died more often from cardiac-related causes such as heart failure or sudden death than the ESRD group (Table 2). Actuarial survival at 2 and 5 years was 66%±7% and 45%±8% in late CKD and 78%±10% and 70%±12% in ESRD compared with 87%±3% and 77%±4%, respectively, in the control group (median survival, 40, 67, and 118 months, respectively; Figure 1). Patients with late CKD had a worse postoperative survival ($P<0.0001$ versus control group), whereas patients with ESRD had nearly comparable overall survival as compared with the control ($P=0.27$ versus control). Similarly, freedom from mortality and readmission for heart failure at 2 and 5 years was 50%±8% and 18%±7% in late CKD ($P<0.0001$ versus control, $P=0.01$ versus ESRD) and 72%±11% and 64%±12% in ESRD ($P=1$ versus control) as compared with 77%±4% and 52%±5%, respectively, in the control group (median event-free survival, 26, 67, and 63 months, respectively; Figure 2).

The Cox proportional hazards model with adjustments for baseline demographics, echocardiographic, and surgical data showed that late CKD (hazard ratio, 2.6; 95% CI, 1.6–4.2;

Table 2. Late Mortality and Morbidity

	Control (n=135)	Late CKD (n=42)	ESRD on HD (n=18)
Late death	22 (16%)	20 (48%)	7 (39%)
Heart failure (LOS)	13	11	0
Sudden death	1	4	0
Infectious disorder	2	2	3
Cerebrovascular accident	1	2	1
Gastrointestinal bleeding	0	0	2
Malignancy	5	0	0
Unknown	0	1	1
Major complications			
Readmission for heart failure	32	12	2
Recurrent MR	7	4	1
Introduction of dialysis	2	5	. . .
Myocardial infarction	2	1	1
Cerebrovascular accident	2	0	0
CRT-D implantation	30	10	2

CKD indicates chronic kidney disease; ESRD, end-stage renal disease; HD, hemodialysis; LOS, low output syndrome; MR, mitral regurgitation; CRT-D, cardiac resynchronization therapy defibrillator.

$P<0.0001$) but not ESRD on hemodialysis (hazard ratio, 1.0; 95% CI, 0.5–2.3; $P=0.91$) was associated with postoperative adverse events defined as mortality and readmission for heart failure.

Pre- and Postoperative Hemodynamic Data

From baseline to 1 month after surgery, LV volumes were substantially decreased in all groups with no intergroup differences in regard to the postoperative values (interaction effects $P>0.05$, group effects $P>0.05$; Figure 3). LVEF changed from 26%±8% to 32%±12%, 25%±7% to 26%±10% and 24%±7± to 33%±8% in the control, late CKD, and ESRD groups, respectively, providing evidence that patients with late CKD showed less improvement in LVEF than the other 2 groups (interaction effect $P=0.027$). LV systolic pressure did not change, whereas LV end-diastolic pressure was decreased in all groups. Systolic and mean PAP were decreased in all groups, whereas right atrial pressure did not change. Cardiac index increased from 2.5±0.7 to 2.8±0.6, 2.4±0.5 to 2.6±0.6, and 2.9±0.7 to 3.1±0.8 L/min/m^2 in the control, late CKD, and ESRD groups, respectively. These findings suggested that improvements in LV function and hemodynamics could be obtained at 1 month after surgery, irrespective of preoperative renal function status, with no substantial intergroup differences for those postoperative values.

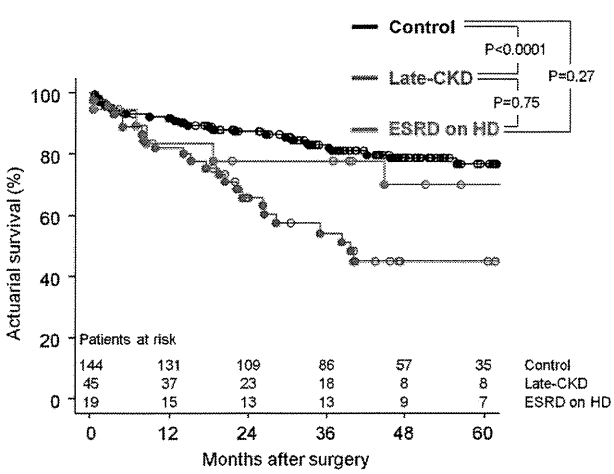

Figure 1. Actuarial survival. CKD indicates chronic kidney disease; ESRD, end-stage renal disease; HD, hemodialysis.

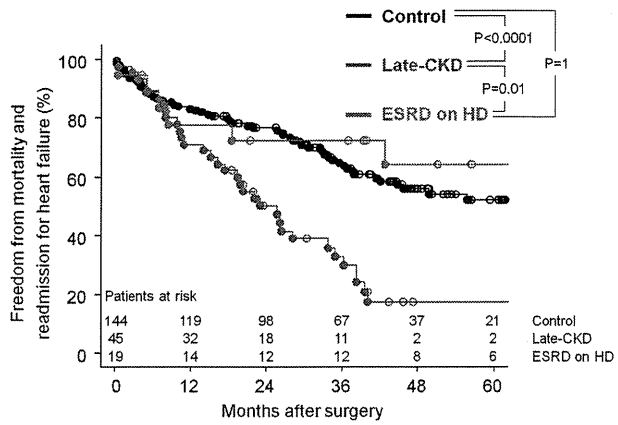

Figure 2. Freedom from mortality and readmission for heart failure. CKD indicates chronic kidney disease; ESRD, end-stage renal disease; HD, hemodialysis.

Serial Echocardiographic Data

LV dimensions were decreased and LVEF was increased at 1 month after surgery in all groups (Figure 4), with subsequent changes in each group apparently distinctive. In the control, these improvements (LV reverse remodeling) persisted during the 2-year follow-up period. As compared with the control group, patients with ESRD showed further decreases in LV dimensions and improvement in LVEF during the follow-up period. In contrast, patients with late CKD showed a gradual reincrease in LV dimensions and less improvement in LVEF than the other groups (interaction effects $P<0.05$ for all).

From baseline to 1 month after surgery, systolic PAP was decreased from 46±13 to 33±11, 49±18 to 35±12, and 49±14 to 34±8 mm Hg in the control, late CKD, and ESRD groups, respectively, showing nearly identical systolic PAP values at 1 month for the 3 groups. The systolic PAP value at 2 years after surgery was 36±14 mm Hg in the control and 33±11 mm Hg in the ESRD group, suggesting that improvement in systolic PAP was nearly completely sustained over time in those 2 groups. In contrast, patients with late CKD showed a gradual reincrease in systolic PAP and had a high PAP value (44±18 mm Hg) at the 2-year follow-up examination.

IVC Dimension

Mean IVC dimension at the latest examination was significantly greater in the late CKD group as compared with the others (Figure 5).

Symptoms and Serial BNP Level

Among patients in 3 study groups, the proportion with New York Heart Association Class I heart failure (no symptoms)

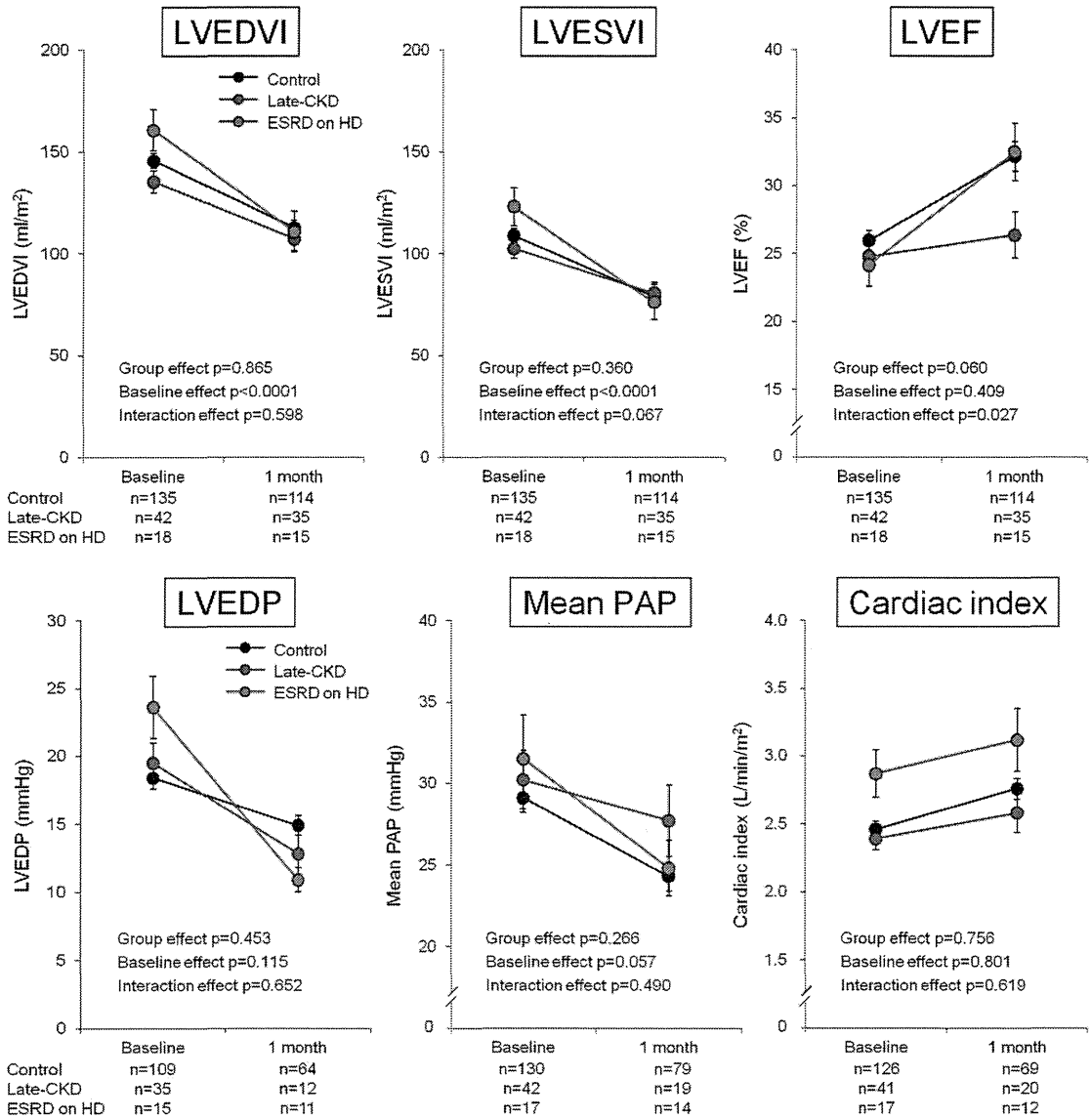

Figure 3. Pre- and postoperative hemodynamic changes. CKD indicates chronic kidney disease; ESRD, end-stage renal disease; HD, hemodialysis; LVEDVI, left ventricular end-diastolic volume index; LVESVI, left ventricular end-systolic volume index; LVEF, left ventricular ejection fraction; LVEDP, left ventricular end-diastolic pressure; PAP, pulmonary artery pressure. Data are presented as mean±SE.

increased and the proportion with Class III or IV heart failure decreased from baseline to the last follow-up visit (91%–15% for the control, 91%–33% for the late CKD, and 95%–17% for the ESRD group, respectively; Figure 6). The symptoms improved by an average of 1.1, 0.7, and 1.2 New York Heart Association classes in the control, late CKD, and ESRD groups, respectively ($P=0.054$ for the difference among the 3 groups in the change from baseline).

Plasma BNP concentration in the control group was decreased at 1 month after surgery and this improvement was sustained during the 2-year follow-up period. As compared with the control, patients with late CKD showed less improvement in plasma BNP value over time, whereas those with ESRD showed remarkable improvement in that value at 1 month and a gradual improvement thereafter (interaction effect $P=0.001$; Figure 7).

Relationship Between IVC Dimension and Plasma BNP Concentration

There was a significant positive correlation between BNP level and IVC dimension at 1 ($r=0.47$, $P<0.0001$) and 2 ($r=0.44$, $P<0.0001$) years after surgery (Figure 8).

Discussion

The major findings can be summarized as follows: (1) restrictive mitral annuloplasty for advanced cardiomyopathy could be performed for high-risk patients with late CKD or ESRD with an acceptable early mortality comparable to that seen in the control; (2) postoperative (1-month) cardiac catheterization resulted in a substantial decrease in LV volume and improvement of hemodynamic status with no intergroup differences for those postoperative values; (3) patients with ESRD had nearly comparable

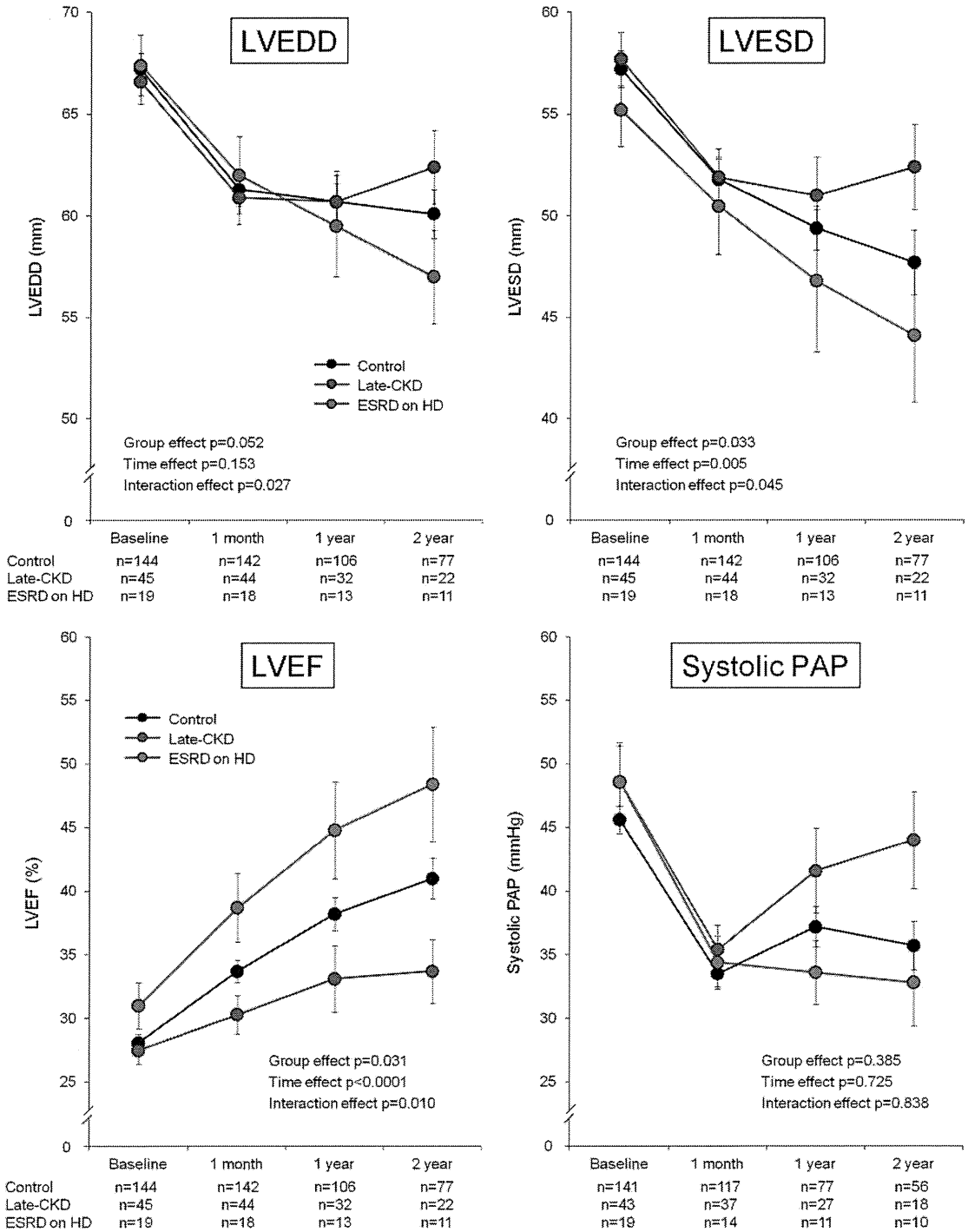

Figure 4. Serial echocardiographic findings. CKD indicates chronic kidney disease; ESRD, end-stage renal disease; HD, hemodialysis; LVEDD, left ventricular end-diastolic dimension; LVEF, left ventricular ejection fraction; LVESD, left ventricular end-systolic dimension; PAP, pulmonary artery pressure. Data are presented as mean±SE.

postoperative outcomes as compared with the control and significantly better outcomes than the late CKD group in terms of freedom from mortality and readmission for heart failure; and (4) patients in the control and ESRD groups showed further improvements in plasma BNP level during the 2-year follow-up period as compared with the late CKD group.

The 5.3% rate of early mortality seen in the patients with ESRD is favorable as compared with that in previous reports, including 20 studies with a total of 863 patients on chronic hemodialysis who underwent various cardiac procedures.[14] Furthermore, the overall survival rate seen in our patients with ESRD is satisfactory given that outcome in patients with heart failure requiring regular hemodialysis is extremely poor with a 3-year survival rate <15% after hospitalization for chronic heart failure.[15]

There are limited data available regarding acute hemodynamic changes after a restrictive annuloplasty in patients with

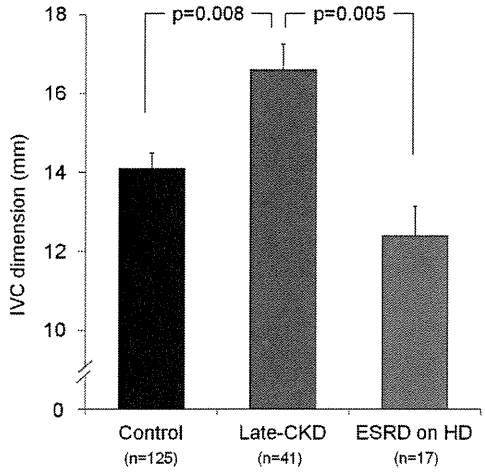

Figure 5. IVC dimension at latest follow-up examination. CKD indicates chronic kidney disease; ESRD, end-stage renal disease; HD, hemodialysis; IVC, inferior vena cava. Comparisons among 3 groups were made using one-way analysis of variance followed by the post hoc pairwise unpaired *t* test. Data are presented as mean±SE.

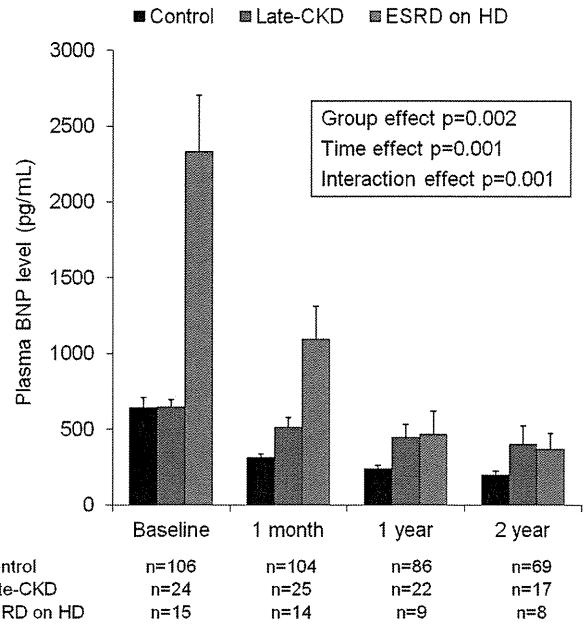

Figure 7. Serial changes in plasma BNP levels. BNP indicates brain natriuretic peptide.

ESRD. Chang et al[16] reported favorable short-term results of 5 patients with chronic hemodialysis undergoing mitral valve repair for "uremic cardiomyopathy" that mimicked the pathophysiological disorder in patients with dilated cardiomyopathy resulting from chronic volume overload. Their echocardiographic findings showed that LV end-diastolic volume decreased from 168±20 at baseline to 113±36 mL, whereas LV end-systolic volume decreased from 91±38 to 52±26 mL after mitral valve repair for uremic cardiomyopathy, similar to that seen in our patients with ESRD. Importantly, cardiac catheterization in the present study allowed confirmation of improvements in LV volume and function as well as other hemodynamic parameters including LV end-diastolic pressure, mean PAP, and cardiac index, irrespective of preoperative renal function status. Furthermore, our serial echocardiographic examinations extending over 2 years revealed that the sustained improvements in LV function (reverse LV remodeling) and hemodynamics seen in patients with ESRD were comparable to those in the control group, indicating the efficacy of surgical intervention in patients with ESRD.

Plasma BNP concentration may be a useful biomarker of heart failure and provide prognostic information.[17] Sustained improvements in BNP level in the control and ESRD groups may indicate that relief of heart failure obtained immediately

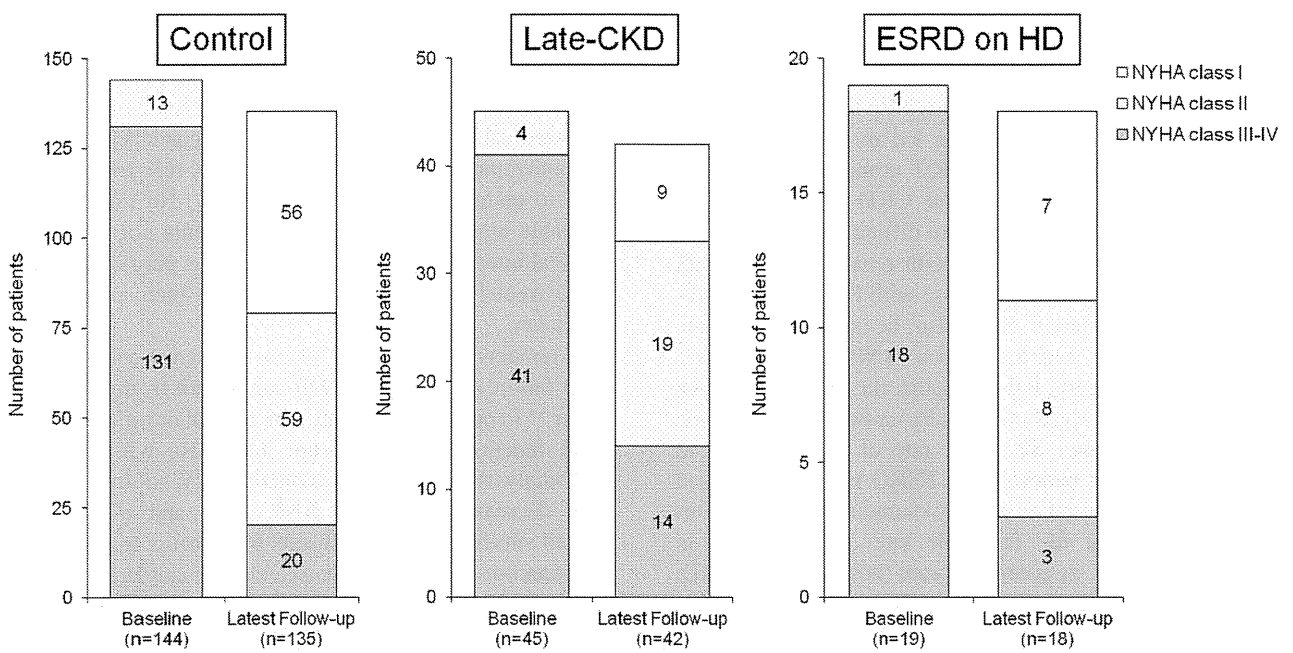

Figure 6. Heart failure symptoms at baseline and at the last follow-up visit. CKD indicates chronic kidney disease; ESRD, end-stage renal disease; HD, hemodialysis.

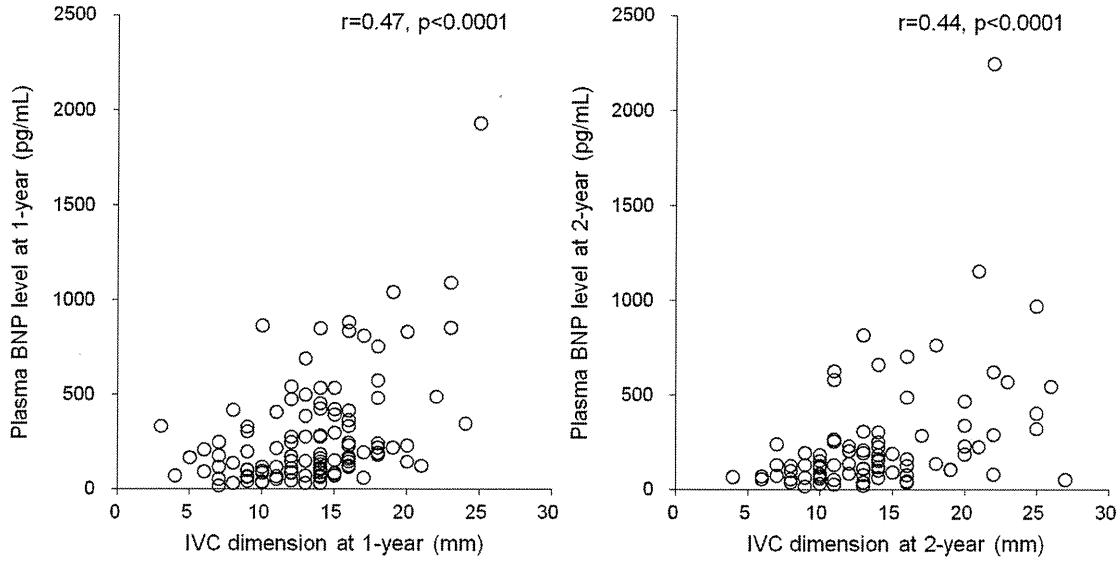

Figure 8. Relationship between IVC dimension and plasma BNP level. CKD indicates chronic kidney disease; ESRD, end-stage renal disease; HD, hemodialysis; IVC, inferior vena cava; BNP, brain natriuretic peptide.

after surgery was sustained over time, possibly accounting for the better outcome than seen in the late CKD group. In contrast, plasma BNP in patients with late CKD was decreased at 1 month after surgery along with a substantial decrease in LV volume confirmed by left ventriculography; however, that value remained substantially high at all follow-up time points, suggesting abnormal hemodynamics and unfavorable functional status despite significant MR improvement in the patients with late CKD.

Finally, we found a significant difference in the late outcome between the late CKD and ESRD groups despite no intergroup differences in postoperative LV and hemodynamic function, except for LVEF. Patients with ESRD exhibited a smaller IVC dimension than those with late CKD at the latest follow-up examination and also had higher rates of freedom from mortality and readmission for heart failure as compared with those with late CKD. Because IVC dimension is an indicator of volume status in patients with heart failure,[10] our findings regarding IVC dimension led us to speculate that volume management for the ESRD group was performed more appropriately than for the late CKD group during the follow-up period. Indeed, it is more difficult to control body fluid volume balance in patients with renal dysfunction not receiving hemodialysis than in those with ESRD on hemodialysis.[18] Our speculation may also be supported by the positive correlation found between BNP level and IVC dimension after surgery, indicating that the increased plasma BNP levels might have been partially caused by LV volume overload. Furthermore, the lower rate of mortality due to heart failure seen in patients with ESRD may be accounted for by adequate fluid removal and volume management. Our data suggested that the favorable late outcome seen in patients with ESRD, as compared with those with late CKD, was not mainly attributed to the surgical intervention itself, but rather adequate postoperative volume management. Therefore, we consider that postoperative volume management is important for better outcome in patients with functional MR and advanced cardiomyopathy; thus careful and meticulous monitoring of volume status is mandatory, especially for patients with late CKD.

Study Limitations

This study was retrospective in nature and investigated a small number of subjects; thus, any conclusions are limited. In particular, the sample size for ESRD on hemodialysis is very small and may have involved biased sampling, which might have led to the result showing no difference in survival between the patients with ESRD and control subjects. Inclusion of patients with different etiologies for heart failure and patients who had undergone concomitant surgical intervention such as coronary artery bypass grafting or surgical ventricular reconstruction might have influenced the results. However, such concomitant procedures are usually required for sick patients with a similar clinical and pathophysiologic status despite the etiology of LV dysfunction. We only analyzed patients with functional MR secondary to advanced cardiomyopathy considered suitable by referring cardiologists to undergo restrictive annuloplasty. No information is available regarding the number of patients not referred for surgical intervention during the same time period, because of the extremely high risk considered by their primary care physician.

It remains controversial whether patients with end-stage heart failure and functional MR can benefit from mitral valve repair.[19] In our study, patients with normal or mildly impaired renal function (control group) and those with ESRD on hemodialysis showed improvements in LV volume and function, decreases in plasma BNP level, and a satisfactory overall survival rates. Our results from meticulous follow-up examinations, including invasive cardiac catheterization at 1 month after surgery as well as sequential BNP levels, show that mitral valve repair improved hemodynamics and symptoms in those patients. However, the lack of an untreated control group did not allow us to investigate the survival

benefit conferred by mitral valve repair in patients with ESRD on hemodialysis. Additional randomized studies with higher numbers of patients and longer follow-up periods are necessary to confirm our results.

Conclusion

Mitral valve repair for medically refractory functional MR and Stage C/D heart failure yielded improvement in LV function and hemodynamics with an acceptably low hospital mortality, irrespective of preoperative renal function status. Patients with ESRD showed favorable late outcome in terms of freedom from mortality and readmission for heart failure as compared with those with late CKD. Further studies are needed to assess the survival benefit of mitral valve repair in patients with end-stage renal disease and advanced heart failure.

Sources of Funding

This study was partially supported by research funds to promote the hospital function of Japan Labor Health and Welfare Organization.

Disclosures

None.

References

1. Kazory A, Ross EA. Contemporary trends in the pharmacological and extracorporeal management of heart failure: a nephrologic perspective. *Circulation.* 2008;117:975–983.
2. Go AS, Chertow GM, Fan D, McCulloch CE, Hsu CY. Chronic kidney disease and the risks of death, cardiovascular events, and hospitalization. *N Engl J Med.* 2004;351:1296–1305.
3. Kottgen A, Russell SD, Loehr LR, Crainiceanu CM, Rosamond WD, Chang PP, Chambless LE, Coresh J. Reduced kidney function as a risk factor for incident heart failure: the Atherosclerosis Risk In Communities (ARIC) study. *J Am Soc Nephrol.* 2007;18:1307–1315.
4. Heywood JT. The cardiorenal syndrome: lessons from the ADHERE database and treatment options. *Heart Fail Rev.* 2004;9:195–201.
5. Levey AS, Stevens LA, Schmid CH, Zhang YL, Castro AF III, Feldman HI, Kusek JW, Eggers P, Van Lente F, Greene T, Coresh J; CKD-EPI (Chronic Kidney Disease Epidemiology Collaboration). A new equation to estimate glomerular filtration rate. *Ann Intern Med.* 2009;150: 604–613.
6. Rahmanian PB, Adams DH, Castillo JG, Vassalotti J, Filsoufi F. Early and late outcome of cardiac surgery in dialysis-dependent patients: single-center experience with 245 consecutive patients. *J Thorac Cardiovasc Surg.* 2008;135:915–922.
7. K/DOQI clinical practice guidelines for chronic kidney disease: evaluation, classification, and stratification. National Kidney Foundation. *Am J Kidney Dis.* 2002;39:1–266.
8. Pepi M, Tamborini G, Galli C, Barbier P, Doria E, Berti M, Guazzi M, Fiorentini C. A new formula for echo-Doppler estimation of right ventricular systolic pressure. *J Am Soc Echocardiogr.* 1994;7:20–26.
9. Kircher BJ, Himelman RB, Schiller NB. Noninvasive estimation of right atrial pressure from the inspiratory collapse of the inferior vena cava. *Am J Cardiol.* 1990;66:493–496.
10. Goonewardena SN, Gemignani A, Ronan A, Vasaiwala S, Blair J, Brennan JM, Shah DP, Spencer KT. Comparison of hand-carried ultrasound assessment of the inferior vena cava and N-terminal pro-brain natriuretic peptide for predicting readmission after hospitalization for acute decompensated heart failure. *J Am Coll Cardiol Cardiovasc Imaging.* 2008;1:595–601.
11. Bolling SF, Pagani FD, Deeb GM, Bach DS. Intermediate-term outcome of mitral reconstruction in cardiomyopathy. *J Thorac Cardiovasc Surg.* 1998;115:381–388.
12. Kitamura S. Excision of left ventricular aneurysm and large scarred myocardium following myocardial infarct: Postoperative and follow-up studies based on hemodynamics and left ventricular function. *Nippon Kyobu Geka Gakkai Zasshi.* 1976;24:1343–1364.
13. Ohara K. Clinical studies concerning surgical indication for excision of left ventricular aneurysm or asynergy following myocardial infarction. *Nippon Kyobu Geka Gakkai Zasshi.* 1977;25:907–927.
14. Horst M, Mehlhorn U, Hoerstrup SP, Suedkamp M, de Vivie ER. Cardiac surgery in patients with end-stage renal disease: 10-year experience. *Ann Thorac Surg.* 2000;69:96–101.
15. Trespalacios FC, Taylor AJ, Agodoa LY, Bakris GL, Abbott KC. Heart failure as a cause for hospitalization in chronic dialysis patients. *Am J Kidney Dis.* 2003;41:1267–1277.
16. Chang JP, Kao CL. Mitral valve repair in uremic congestive cardiomyopathy. *Ann Thorac Surg.* 2003;76:694–697.
17. Zoccali C, Mallamaci F, Benedetto FA, Tripepi G, Parlongo S, Cataliotti A, Cutrupi S, Giacone G, Bellanuova I, Cottini E, Malatino LS; Creed Investigators. Cardiac natriuretic peptides are related to left ventricular mass and function and predict mortality in dialysis patients. *J Am Soc Nephrol.* 2001;12:1508–1515.
18. Takami Y, Horio T, Iwashima Y, Takiuchi S, Kamide K, Yoshihara F, Nakamura S, Nakahama H, Inenaga T, Kangawa K, Kawano Y. Diagnostic and prognostic value of plasma brain natriuretic peptide in non-dialysis-dependent CRF. *Am J Kidney Dis.* 2004;44:420–428.
19. Wu AH, Aaronson KD, Bolling SE, Pagani FD, Welch K, Koelling TM. Impact of mitral valve annuloplasty on mortality risk in patients with mitral regurgitation and left ventricular systolic dysfunction. *J Am Coll Cardiol.* 2005;45:381–387.

Biomaterials 34 (2013) 662–668

Contents lists available at SciVerse ScienceDirect

Biomaterials

journal homepage: www.elsevier.com/locate/biomaterials

Network formation through active migration of human vascular endothelial cells in a multilayered skeletal myoblast sheet

Eiji Nagamori [a], Trung Xuan Ngo [b], Yasunori Takezawa [b], Atsuhiro Saito [c], Yoshiki Sawa [c], Tatsuya Shimizu [d], Teruo Okano [d], Masahito Taya [b], Masahiro Kino-oka [a,*]

[a] Department of Biotechnology, Graduate School of Engineering, Osaka University, 2-1 Yamada-oka, Suita, Osaka 565-0871, Japan
[b] Division of Chemical Engineering, Graduate School of Engineering Science, Osaka University, 1-3 Machikaneyama-cho, Toyonaka, Osaka 560-8531, Japan
[c] Department of Surgery, Division of Cardiovascular Surgery, Graduate School of Medicine, Osaka University, 2-15 Yamada-oka, Suita, Osaka 565-0871, Japan
[d] Institute of Advanced Biomedical Engineering and Science, Tokyo Women's Medical University, 8-1 Kawada-cho, Shinjuku-ku, Tokyo 162-8666, Japan

ARTICLE INFO

Article history:
Received 10 August 2012
Accepted 23 August 2012
Available online 30 October 2012

Keywords:
Cell sheet
Vascular endothelial cells
Skeletal myoblasts
Angiogenesis
Cell migration
Image processing

ABSTRACT

Autologous transplantation of myoblast sheet has attracted attention as a new technique for curing myocardial infarction. Myoblast sheet has the ability to secret cytokines that improve heart function via the facilitation of angiogenesis on affected part. To mimic the *in vivo* angiogenesis in the myoblast sheet after transplantation, a five-layered cell sheet of human skeletal muscle myoblasts (HSMMs) was overlaid on human umbilical vein endothelial cells (HUVECs) which enables evaluation of dynamic HUVEC behavior. HUVECs existing initially at the bottom of the sheet changed to be a stretched shape and migrated upward compared with the surrounding HSMMs in the sheet. Prolonged incubation resulted in network formation of HUVECs in the middle of the sheet, although non-networked HUVECs continued to migrate to the top of the sheet, which meant the spatial habitation of HUVECs in the cell sheet. Image processing was performed to determine the variation in the extent of network formation at different HUVEC densities. It was found that the extent of formed network depended on the frequency of encounters among HUVECs in the middle of the sheet. The present system, which can evaluate network formation, is considered to be a promising *in vitro* angiogenesis model.

1. Introduction

Cell sheet engineering has been proposed to be a promising technique to form plate-shaped aggregates, which are thought to mimic tissues available for transplantation [1]. A temperature-responsive poly-(*N*-isopropylacrylamide) (PNIPAAm)-grafted surface can be used to harvest a cell sheet without enzymatic digestion of the intact extracellular matrix on the detached surface [2] to enable the construction of three-dimensional (3-D) multi-layered tissues without scaffolds [3].

Recently, autologous transplantation of myoblast sheet has attracted attention as a new technique for curing myocardial infarction, which is associated with cardiomyocyte dysfunction and irreversible cell loss [4,5]. Skeletal myoblasts, which are relatively easy to harvest from patients, can undergo self-renewal and differentiation, allowing cardio muscle regeneration upon injury. Myoblast sheet also has the ability to secret cytokines that improve heart function via the facilitation of angiogenesis and attraction of progenitors on affected part. The sheet transplantation method can overcome disadvantages of the myoblast injection method, such as loss of transplanted cells due to poor survival of cells [6] and arrhythmic heart beat due to a global down-regulation of connexin 43 in the host heart [7]. Sawa et al. conducted the first clinical trial of the transplantation using myoblast sheet that enables the effective delivery of a sheet for a large coverage area to provide the improvement of damaged heart function *in vivo* without arrhythmic heart beats [8]. Further development of transplantation using the multilayered myoblast sheets showed the improved heart function when compared with monolayer sheet transplantation [9].

From a manufacturing point of view, process and quality controls are important for realizing commercialization of cell sheet transplant. Many studies have addressed cell sources, culture, sheet assembling, and *in vivo* animal tests; however, the method for quality control of myoblast sheets, especially for transplant efficacy such as angiogenesis capability, has not been systematized. Although animal tests can be used to estimate the overall efficacy of the transplants, such methods provide an insufficient estimation

* Corresponding author. Tel.: +81 (0) 6 6879 7444; fax: +81 (0) 6 6879 4246.
E-mail address: kino-oka@bio.eng.osaka-u.ac.jp (M. Kino-oka).

0142-9612/$ – see front matter © 2012 Elsevier Ltd. All rights reserved.
http://dx.doi.org/10.1016/j.biomaterials.2012.08.055